ShhN-mediated activation of Smo in the absence of Ptch1/2 function

Catalina Casillas and Henk Roelink

Department of Molecular and Cell Biology, 16 Barker Hall, 3204, University of California, Berkeley CA 94720, USA

roelink@berkeley.edu

Abstract

Contrary to the canonical model of Hh signaling, we find that cells genetically lacking *Ptch1* and *Ptch2* remain responsive to ShhN. These cells retain the ability to migrate towards a source of ShhN, while expression of ShhN results in a robust activation of the transcriptional Hh response; both occur in a Smo-dependent manner. This activation of Hh responses does not require binding to the co-receptors Boc, Cdo, or Gas1, nor Shh autocatalytic processing, as the cholesterol moiety on Shh impedes signaling. Shh mutants unable to bind their cognate receptors, or fail to undergo proper processing, nevertheless retain their ability to activate the Hh response both in vivo and in vitro. Together, our findings support a model in which the role of Ptch1/2 as an inhibitor of Smo intersects with a Shh-mediated Smo activation event that is independent of known Shh receptors.

Introduction

Sonic Hedgehog (Shh) is a signaling molecule indispensable for vertebrate embryonic development and adult stem cell niche maintenance (Ingham and McMahon, 2001). Impaired regulation of the Hedgehog (Hh) pathway is a known cause of various birth defects and diseases (Bale, 2002).

In the absence of the Hh ligands, the receptors Patched1 (Ptch1) and Patched2 (Ptch2) inhibit the signal transducer Smoothened (Smo) through a sub-stoichiometric mechanism (Alfaro et al., 2014; Taipale et al., 2002; Zhang et al., 2001a). Ptch1/2 belong to the Resistance, Nodulation, and Division (RND) family of transmembrane transporters, and their inhibition requires the putative proton anti-porter activity that characterizes these molecules (Taipale et al., 2002). In general, RNDs mediate the secretion of small lipophilic and amphipathic molecules (Nikaido and Zgurskaya, 2001; Nikaido and Takatsuka, 2009), and it has been proposed that Ptch1/2 re-localize a sterol that modifies Smo activity (Huang et al., 2016; Taipale et al., 2002).

The binding of extracellular Shh requires Ptch1/2 in conjunction with the co-receptors, Boc, Cdo, and Gas1 (Allen et al., 2011; Izzi et al., 2011; Marigo et al., 1996). Shh is internalized during signaling, causing a change in the subcellular distribution and activity of Smo (Aanstad et al., 2009; Bijlsma et al., 2012; Incardona et al., 2002; 2000; Milenkovic et al., 2009). How these events regulate Smo activity remains unclear. The Hh pathway is upregulated in *Ptch1* null mice and neuralized *Ptch1*$^{LacZ/LacZ}$*;Ptch2*$^{-/-}$ mouse embryonic stem cells, supporting the canonical model that Smo activity is principally regulated by changes in Ptch1/2-mediated inhibition (Alfaro et al., 2014; Goodrich et al., 1997). A tenet of this model is that Smo is constitutively active in the absence of Ptch1/2 function.

Smo is a Class F G-protein coupled receptor (GPCR) and belongs to the superfamily of receptors predominantly defined by Frizzleds (Frz), the canonical receptors of the Wnt signaling pathway (Bhanot et al., 1996; Kristiansen, 2004). Smo and Frzs share over 25% sequence identity and harbor a conserved extracellular, amino-terminal Cysteine Rich Domain (CRD) and seven hydrophobic domains. The CRD of Frz binds to Wnt through two distinct binding sites, one of which is a protein-lipid interface, to initiate signal transduction (Janda et al., 2012). Similarly, the CRD of Smo has been shown to bind to a variety of sterols (Myers et al., 2013; Nachtergaele et al., 2013; Nedelcu et al., 2013), including cholesterol (Huang et al., 2016), which can modulate Smo activity. Smo can also be regulated by small molecule agonists and antagonists that target its membrane-exposed heptahelical domain. This heptahelical domain of Smo is thought to be the target of the inhibitory effect of Ptch1 (Chen et al., 2002a; 2002b; Wang and McMahon, 2013).

Our results support earlier observations that Smo activity can be regulated in a Ptch1/2 independent manner, by demonstrating that ShhN can mediate the activation of Smo in cells lacking Ptch1/2.

Ptch1 and Ptch2 are dispensable for a cell's ability to migrate towards a source of ShhN, a Hh response that nevertheless requires Smo. Although exogenously supplied ShhN does not induce a transcriptional Hh response in cells lacking Ptch1/2, transfection of *ShhN* causes a significant Smo-dependent activation of the transcriptional response. The mechanism regulating cell-autonomous Smo activation is fundamentally different from non-cell autonomous activation via the canonical Shh receptors. Shh mutants unable to bind to canonical Hh receptors, or unable to undergo post-translational processing, retain their ability to induce the Hh response after expression in cells lacking Ptch1/2, as well as after expression in the developing neural tube. Our work reveals a more complex model of Shh signal transduction in which the role of Ptch1 as a catalytic inhibitor of Smo activity intersects with a relatively direct interaction between Shh and Smo, together regulating the definitive level of pathway activation.

Results

The CRD of Smo is not required for its inhibition by Ptch1/2

Sterols have long been proposed to be the cargo which Ptch1 transports across membranes to regulate Smo activity, leaving open the possibility that the CRD of Smo is the target of Ptch1 function. While this issue remains unresolved, it has been shown that a form of Smo lacking its CRD (SmoΔCRD) has reduced sensitivity to Shh signaling (Myers et al., 2013; Nachtergaele et al., 2013) and increased constitutive activity (Byrne et al., 2016). To determine whether Ptch1 targets the CRD of Smo, we used *Ptch1*$^{LacZ/LacZ}$;*Ptch2*$^{-/-}$ fibroblasts derived from mouse embryonic stem cells (mESCs) (Roberts et al., 2016) to assess Ptch1 function in the absence of endogenous Ptch1/2 activity. Transfection of either *Smo* or *SmoΔCRD* into *Ptch1*$^{LacZ/LacZ}$;*Ptch2*$^{-/-}$ cells moderately raised the level of Hh pathway activity (Figure 1A), measured using a well-characterized *Gli-Luciferase* reporter (Taipale et al., 2002). Co-transfection of *Smo* or *SmoΔCRD* together with *Ptch1* or *Ptch1ΔL2* (a dominant inhibitory form of Ptch1 (Briscoe et al., 2001)), predictably lowered Hh pathway activity caused by *Smo* expression. However, co-transfection of *Smo* or *SmoΔCRD* with forms of Ptch1 that contain mutations within the putative antiporter domain, *Ptch1D499A* and *Ptch1ΔL2-D499A*, were less effective at inhibiting the Hh pathway activity caused by *Smo* overexpression (Figure 1A). Thus Smo, including forms lacking its CRD, remains subject to the inhibitory effects of the proton antiporter activity of Ptch1, demonstrating that the CRD of Smo is not the target of Ptch1-mediated inhibition.

To verify our observation *in vivo*, we assessed the ability of Ptch1 to inhibit SmoΔCRD in the developing embryo. Electroporation of the chick neural tube is a well-established procedure to introduce transgenes into a normally developing embryo (Itasaki et al., 1999). Electroporation of *Smo* into stage 10-11 (Hamburger and Hamilton, 1951) chick neural tubes did not affect the Hh response pathway (Figure 1B-D). However, electroporation of *SmoΔCRD* resulted in an expansion of the ventral neural markers Nkx2.2 and Mnr2 (Figure1E-G), indicative of an ectopic activation of the Hh response pathway. Intrinsic activation of *SmoΔCRD* has been observed before (Byrne et al., 2016), which indicates that the CRD of Smo is able to regulate its downstream activity. We find that the activity of SmoΔCRD remains subject to Ptch1-mediated inhibition *in vivo* as well, as electroporation of *SmoΔCRD* together with *Ptch1ΔL2*, reversed the phenotypic effects of *SmoΔCRD* expression (Figure 1H-J). SmoΔCRD has been shown to constitutively localize to the primary cilium, the cellular compartment where it mediates the transcriptional Hh response (Aanstad et al., 2009). The entry of Smo into the cilium is required for transcriptional pathway activation, and we find that electroporation of a form of SmoΔCRD that cannot localize to the primary cilium, *SmoΔCRD-CLD* (Aanstad et al., 2009; Corbit et al., 2005), did not result in ectopic activation of the pathway *in vivo* (Figure 1K-M). These results demonstrate that the CRD of Smo is not required for its inhibition by Ptch1, and thus lends support to the idea that the heptahelical domain of Smo is the target for Ptch1 inhibition.

SmoΔCRD is intrinsically active *in vivo* (Figure 1E-G), while the activity of Smo and SmoΔCRD in *Ptch1*$^{LacZ/LacZ}$;*Ptch2*$^{-/-}$ cells is indistinguishable (Figure 1A). To evaluate Smo activity in cells lacking all Ptch activity, we derived fibroblasts from *Ptch1*$^{LacZ/LacZ}$;*Ptch2*$^{-/-}$;*Smo*$^{-/-}$ mESCs (Robertson et al., 2016). We assessed the intrinsic activity of Smo and its mutant derivatives in these cells by transfecting the *Gli-Luciferase* reporter with *Smo*, *SmoΔCRD*, *SmoΔCRD-CLD*, *SmoM2* (an intrinsically active mutant (Xie et al., 1998)), *SmoL112D-W113Y* (a mutant unable to bind sterols within the CRD (Nachtergaele et al., 2013)), or *Drosophila Smo*. Remarkably, none of these mutant forms of Smo induced the Hh response better than wild type (Figure 1N). Overall, SmoΔCRD-CLD, SmoL112D-W113Y and Drosophila Smo were less able to induce the transcriptional Hh response compared to Smo, *SmoΔCRD*, and SmoM2 (Figure 1N). This observation is consistent with the notion that SmoM2 is refractory to Ptch1/2 regulation, and suggests that an additional activation event may be required to further induce a Hh response.

We next tested whether we could further modulate Smo activity with SAG, an agonist that targets the heptahelical domain, in the absence of Ptch1/2 activity. We measured the Hh response using both the *Gli-Luciferase* reporter and the endogenous *Ptch1:LacZ* reporter contained within *Ptch1*$^{+/LacZ}$ and *Ptch1*$^{LacZ/LacZ}$;*Ptch2*$^{-/-}$ fibroblasts. We found that both transcriptional reporters revealed identical results; *Ptch1*$^{LacZ/LacZ}$;*Ptch2*$^{-/-}$ cells were completely insensitive to SAG, a powerful activator of Smo

in cells that retain Ptch1/2 activity (Figure 1O). These results indicate that Ptch1/2 function is required for SAG-mediated activation of Smo; and thus might act as an antagonist to the inhibitory activity of Ptch1.

ShhN can activate the Hh pathway independent of Ptch1/2 function

As a central ligand in the activation of the Hh response, we assessed whether Shh can affect Smo activity in the absence of Ptch1/2. We have previously demonstrated that Shh-mediated chemotaxis involves the activation of Smo that is quick (in the order of minutes), independent of the primary cilium (Bijlsma et al., 2012), and independent of Ptch1 (Alfaro et al., 2014); leaving open the possibility that Ptch2 serves as the primary receptor. We tested the ability of *Ptch1*$^{LacZ/LacZ}$;*Ptch2*$^{-/-}$ fibroblasts to migrate towards a localized source of ShhN (a soluble form of Shh) using a modified Boyden chamber (Chen, 2005). We found that *Ptch1*$^{LacZ/LacZ}$;*Ptch2*$^{-/-}$ cells were indistinguishable from *Ptch1*$^{LacZ/LacZ}$ cells in their ability to migrate towards ShhN (Figure 2A). Shh chemotaxis was largely abolished in *Ptch1*$^{LacZ/LacZ}$;*Ptch2*$^{-/-}$;*Smo*$^{-/-}$ cells, although these cells were retained the ability to migrate towards FCS, our positive control (Figure 2A). These results demonstrate that all Ptch1/2 function is dispensable for the activation of Smo by exogenous ShhN. As the Shh co-receptor Boc has been implicated in the Shh-mediated guidance of commissural growth cones towards the floor plate (Okada et al., 2006), we made a fibroblast line that, besides Ptch1/2, also lack Boc, its paralog Cdo, as well as the co-receptor Gas1. We found that *Ptch1*$^{LacZ/LacZ}$;*Ptch2*$^{-/-}$;*Shh*$^{-/-}$;*Boc*$^{-/-}$;*Cdo*$^{-/-}$;*Gas1*$^{-/-}$ cells, like all cell lines tested, retain their ability to migrate towards FCS; however, their ability to migrate towards ShhN is impaired, but not completely abolished (Figure 2A).

These findings are not readily reconciled with our earlier observation that *Ptch1*$^{LacZ/LacZ}$;*Ptch2*$^{-/-}$ cells cannot upregulate the transcriptional Hh response when exposed to exogenous ShhN, unless transfected with *Ptch1* (Roberts et al., 2016). Since Ptch1 mediates the internalization of Shh during signaling (Incardona et al., 2000), we tested whether we could circumvent this function of Ptch1 by providing ShhN intracellularly through transfection of a *ShhN* construct. Using a panel of cell lines lacking various combinations of *Ptch1* and *Ptch2*, we found that transfection of *ShhN* invariably induced an upregulation of the transcriptional Hh response regardless of the presence or absence of Ptch1/2 (Figure 2B, C). The induction of the Hh response was measured using both a transfected *Gli-Luciferase* reporter (Figure 2B), as well as the genetically encoded *Ptch1:LacZ* reporter (Goodrich et al., 1997) (Figure 2C). The finding that *Ptch1*$^{LacZ/LacZ}$;*Ptch2*$^{-/-}$ cells cannot activate the transcriptional Hh pathway in response to extracellular ShhN indicates that signaling is occurring intracellularly in cells lacking Ptch1/2, and is not the result of non-cell autonomous signaling;

henceforth we will refer to this as “cell-autonomous activation”. In all cases, we found that the Smo specific inhibitor Vismodegib (Rudin, 2012) significantly blocked the induction, demonstrating that the transcriptional Hh response caused by *ShhN* transfection is mediated by Smo (Figure 2B, C). We found a high level of cilial occupation by Smo:GFP (Figure 2D) in *Ptch1*$^{LacZ/LacZ}$;*Ptch2*$^{-/-}$ cells, consistent with earlier observations in *Ptch1*$^{-/-}$ cells (Rohatgi et al., 2007). Transfection of *ShhN* in *Ptch1*$^{LacZ/LacZ}$;*Ptch2*$^{-/-}$ cells caused a small, but significant increase in the cilial occupation of Smo::GFP (Figure 2D), a demonstrated output of the transcriptional Hh response. Together these results demonstrate that ShhN can mediate activation of the Hh response pathway via a mechanism that does not require Ptch1/2 function.

We found that the *Ptch1*$^{LacZ/LacZ}$ fibroblast cell line has a higher level of intrinsic pathway activity compared to the *Ptch1*$^{LacZ/LacZ}$;*Ptch2*$^{-/-}$ cell line, as measured by both the *Gli-luciferase* and *Ptch1:LacZ* reporters (Figure 2, Figure Supplement 1). Our results that Vismodegib treatment lowers the basal level of pathway activity in *Ptch1*$^{LacZ/LacZ}$ cells is consistent with this observation. However, the induction of transcriptional pathway activity caused by *ShhN* transfection in *Ptch1*$^{LacZ/LacZ}$ cells, as well as the ability of these cells to migrate towards a source ShhN, demonstrate that the absence of Ptch1 does not result in full activation of the Hh response; necessitating additional mechanisms by which Smo can be activated in the absence of Ptch1. The *Ptch1*$^{LacZ/LacZ}$ fibroblast line was derived from mutant embryos, while we derived the compound mutant fibroblast line from embryonic stem cells. The methods by which these cells were derived may explain the differences in their basal level of Hh pathway activity; epigenetically, these cells are expected to be quite different. This notion is supported by the characteristics of a Ptch1 null, Ptch2 containing fibroblast line (*Ptch1*$^{-/-}$;*Disp1*$^{-/-}$;*Shh*$^{-/-}$) we derived from mESCs; which, unlike the *Ptch1*$^{LacZ/LacZ}$ line, retains a low level of intrinsic pathway activity similar to the *Ptch1*$^{LacZ/LacZ}$;*Ptch2*$^{-/-}$ cell line, however remains equally sensitive to *ShhN* transfection (Figure 2B).

Despite differences in the levels of endogenous Hh pathway activity, we found that co-transfection of *Gli-Luc* with *Ptch1* or *Ptch1ΔL2* effectively inhibited the transcriptional Hh pathway in both *Ptch1*$^{LacZ/LacZ}$ and *Ptch1*$^{LacZ/LacZ}$;*Ptch2*$^{-/-}$ cells (Figure 2, Figure Supplement 2A). Forms of Ptch1 lacking the putative antiporter function, Ptch1D499A and Ptch1ΔL2-D499A, were less effective inhibitors of the Hh response pathway than their antiporter-competent counterparts. Transfection of *Gli3*^{PHS}, a dominant inhibitory form of Gli3 (Meyer and Roelink, 2003), efficiently repressed the level of Hh pathway activity in both cells lines (Figure 2, Figure Supplement 2A), while overexpression of *Gli1* caused a significant 10-fold induction (data not shown). These results demonstrate that, regardless of the basal state of the pathway, both cells lines predictably respond to inhibitory elements and thus retain all of the proper components of Hh pathway regulation. To test whether the

transcriptional Hh response caused by ShhN transfection is subject to the same regulation, we co-transfected *ShhN* with either *Ptch1ΔL2 or Gli3*^{PHS}. We found that the induction caused by *ShhN* transfection was inhibited by Ptch1ΔL2, demonstrating that ShhN-activated Smo remains subject to Ptch1 inhibition in both *Ptch1*$^{LacZ/LacZ}$ and *Ptch1*$^{LacZ/LacZ}$;*Ptch2*$^{-/-}$ cells (Figure 2, Figure Supplement 2B). The relative decrease of Smo activity caused by Ptch1 inhibition is similar under all conditions, which supports the idea that Ptch1 is a non-competitive inhibitor of Smo activation by ShhN. Similarly, *Gli3*^{PHS} was able to repress the induction caused by *ShhN* transfection, implicating the canonical Gli transcription factors as the mediators of this Hh response. These results validate the Gli-Luciferase reporter as a faithful representation of the state of the Hh pathway in these cells.

Ptch1/2-independent cell-autonomous activation of the Hh response does not require Boc, Cdo or Gas1

Boc, Cdo, and Gas1 have been shown to function in an overlapping manner as obligate Shh co-receptors with Ptch1/2 during non-cell autonomous Hh signaling (Allen et al., 2011; Izzi et al., 2011; Tenzen et al., 2006). The observation that Ptch1 and Ptch2 are dispensable for the activation of Smo after *ShhN* transfection raises the question whether the Shh co-receptors are involved in detecting ShhN in cells independently of Ptch1/2 during cell-autonomous signaling. We addressed the requirement for Boc, Cdo and Gas1 in two complementary ways. 1) We assessed whether Shh mutants unable to bind to the co-receptors could activate the Hh response cell-autonomously, and 2) we tested whether cells lacking the co-receptors remained sensitive to *ShhN* transfection.

ShhN-E90A, a previously characterized ShhN mutant, cannot bind to either Boc, Cdo, or Gas1, and is unable to activate the Hh response when applied to wildtype cells (Izzi et al., 2011). To independently assess the requirement of Ptch1/2 binding in cell-autonomous pathway activation, we utilized a ShhN mutant with a disrupted zinc coordination site predicted to perturb Ptch1 binding, ShhN-H183A (Fuse et al., 1999; Goetz et al., 2006). We first tested the ability of ShhN-E90A and ShhN-H183A to signal non-cell autonomously (*in trans*), by transfecting *Ptch1* and *Gli-Luc* into *Ptch1*$^{LacZ/LacZ}$;*Ptch2*$^{-/-}$ "reporter" cells and co-culturing them with *Ptch1*$^{LacZ/LacZ}$;*Ptch2*$^{-/-}$ cells independently transfected with *ShhN*, *ShhN-E90A*, or *ShhN-H183A* (Figure 3A, seafoam green). We confirmed our earlier observations that Ptch1-expressing *Ptch1*$^{LacZ/LacZ}$;*Ptch2*$^{-/-}$ reporter cells activated the Hh response when co-cultured with *ShhN* expressing cells (Figure 3C). Reporter cells did not activate the Hh response when cultured with *ShhN-E90A* expressing cells (Figure 3C), corroborating previously published data that ShhN-E90A is unable to mediate Hh signaling *in trans* (Izzi et al., 2011). Consistent with its predicted inability to bind to Ptch1, we find that ShhN-H183A

did not activate the Hh response in reporter cells (Figure 3C). These results support previous observations that activation of the transcriptional response by ShhN in the extracellular space (*in trans* signaling) requires the binding of Shh to Ptch1/2 in conjunction with the co-receptors.

ShhN is a widely used mutant form of Shh, it is freely soluble while retaining its inductive properties (Bumcrot et al., 1995a; Roelink et al., 1995). A significant distinction between ShhN and fully matured Shh is that Shh has a cholesterol moiety that serves as a membrane anchor (Yang et al., 1997). The distinct differences in distribution and extracellular transport between cholesterol-modified and soluble forms of Shh might have significant ramifications for their activities. This led us to test the ability of Shh and mutant derivatives expected to be cholesterol-modified (ShhE90A and ShhH183A) to signal *in trans*. *Ptch1*$^{LacZ/LacZ}$;*Ptch2*$^{-/-}$ reporter cells (transfected with *Gli-Luc* and *Ptch1*) activated the Hh response pathway when co-cultured with Shh and ShhE90A expressing cells, but not with ShhH183A expressing cells (Figure 3E). This result indicates that the cholesterol modification of Shh is able to compensate for the inability to bind Cdo, Boc or Gas1 when signaling *in trans*. The inability of ShhH183A to signal *in trans* may be due, in part, to its poor autocatalytic cleavage, which is directly linked to its modification with a cholesterol moiety (Figure 3B) (Goetz et al., 2006).

We assessed the role of co-receptor binding during cell-autonomous Hh signaling by transfecting mutant forms of *ShhN*, *ShhN-E90A* and *ShhN-H183*, into *Ptch1*$^{LacZ/LacZ}$;*Ptch2*$^{-/-}$ cells together with the *Gli-Luc* reporter (Figure 3A, lilac). We found that, similar ShhN, both ShhN-E90A and ShhN-H183A significantly activated the Hh pathway in *Ptch1*$^{LacZ/LacZ}$;*Ptch2*$^{-/-}$ cells (Figure 3D); indicating that neither Boc, Cdo, nor Gas1 are required for cell-autonomous pathway activation. We next evaluated whether the cholesterol modification on Shh mutants affects cell-autonomous pathway activation by transfecting *Shh* constructs together with the *Gli-Luc* reporter in *Ptch1*$^{LacZ/LacZ}$;*Ptch2*$^{-/-}$ cells (Figure 3A, lilac). We found that transfection of *Shh* into *Ptch1*$^{LacZ/LacZ}$;*Ptch2*$^{-/-}$ cells results in a minute increase of pathway activity (Figure 3F), suggesting that the cholesterol modification on Shh is a major impediment to cell-autonomous activation of the Hh response. In contrast, transfection of *ShhE90A* or *ShhH183A* resulted in a significantly greater pathway induction (Figure 3F). The poor autoproteolysis observed with ShhH183A, which would prevent its cholesterol modification, makes this result difficult to interpret; however, all together these results suggest that Shh interaction with Boc, Cdo or Gas1 impedes cell-autonomous Hh signaling with cholesterol-modified Shh. We confirmed that transfection of these Shh mutants activates a cell-autonomous Hh response in *Ptch1*$^{LacZ/LacZ}$ in a manner similar to *Ptch1*$^{LacZ/LacZ}$;*Ptch2*$^{-/-}$ cells (Figure 3, Figure Supplement 1); again we found that wildtype Shh is a poor inducer of cell-autonomous pathway activation compared to its mutant counterparts.

To further verify the observation that Boc, Cdo and Gas1 are not a required component of the cell-autonomous Hh response, we generated a *Ptch1*$^{LacZ/LacZ}$;*Ptch2*$^{-/-}$;*Boc*$^{-/-}$;*Cdo*$^{-/-}$;*Gas1*$^{-/-}$;*Shh*$^{-/-}$ mESC line and a derived fibroblast line of the same genotype. Upon differentiation into neuralized embryoid bodies, these cells behave similarly to their parental *Ptch1*$^{LacZ/LacZ}$;*Ptch2*$^{-/-}$;*Shh*$^{-/-}$ line (Roberts et al., 2016), and express ventral neural markers indicative of an activated Hh response (Figure 3G). The neural phenotype of differentiated *Ptch1*$^{LacZ/LacZ}$;*Ptch2*$^{-/-}$;*Boc*$^{-/-}$;*Cdo*$^{-/-}$;*Gas1*$^{-/-}$;*Shh*$^{-/-}$ mESCs demonstrates that pathway activation in these cells does not require expression of Shh or the Shh (co-)receptors. Transfection of *ShhN* or any other *Shh* mutant into *Ptch1*$^{LacZ/LacZ}$;*Ptch2*$^{-/-}$;*Boc*$^{-/-}$;*Cdo*$^{-/-}$;*Gas1*$^{-/-}$;*Shh*$^{-/-}$ fibroblasts cells induced a significant increase of the Hh response (Figure 3H). The independently derived *Ptch1*$^{LacZ/LacZ}$;*Ptch2*$^{-/-}$;*Boc*$^{-/-}$;*Cdo*$^{-/-}$;*Gas1*$^{-/-}$;*Shh*$^{-/-}$ and *Ptch1*$^{LacZ/LacZ}$;*Ptch2*$^{-/-}$ fibroblasts behave nearly indistinguishably in this assay.

To assess whether cell-autonomous pathway activation is a phenomenon that occurs across all Hh paralogs, we tested the ability of Indian Hedgehog (Ihh) and Desert Hedgehog (Dhh) to activate the Hh pathway after transfection. The soluble forms IhhN and DhhN are similar to ShhN in their ability to induce the Hh response cell-autonomously, whereas wildtype Ihh and Dhh are significantly more potent than Shh (Figure 3I). These findings demonstrate that cell-autonomous pathway activation is a characteristic of all vertebrate Hedgehog paralogs.

Together our data confirms that the extracellular receptors Boc, Cdo, and Gas1 are not required for pathway activation mediated by *ShhN* expression in Ptch1/2 null cells. As we found before in *Ptch1*$^{LacZ/LacZ}$;*Ptch2*$^{-/-}$ cells (Figure 3F), expression of wild type Shh in *Ptch1*$^{LacZ/LacZ}$;*Ptch2*$^{-/-}$;*Boc*$^{-/-}$;*Cdo*$^{-/-}$;*Gas1*$^{-/-}$;*Shh*$^{-/-}$ only marginally induces the Hh pathway, a further demonstration that the cholesterol moiety prevents cell autonomous signaling by Shh (Figure 3I). This result demonstrates that it is not Boc/Cdo/Gas1 binding that impedes cell-autonomous activation by cholesterol-modified Shh; further analysis is required to understand the activity of ShhE90A

Shh mutants unable to bind to canonical receptors induce the Hh response in the developing neural tube

Both Ptch1 and Ptch2, as well as Boc, Cdo, and Gas1 have been shown to play central roles in regulation of the Hh responses *in vivo* (Allen et al., 2011; Goodrich et al., 1997; Izzi et al., 2011). We assessed whether expression of Shh mutants can activate the Hh response independent of (co)-receptor interaction in the developing neural tube of chicken embryos. We electroporated stage 10-11 (Hamburger and Hamilton, 1951) chick neural tubes with *ShhN*, *ShhN-E90A*, or *ShhN-H183* together with *GFP*. We found that all ShhN mutants are able to activate the Hh pathway as assessed

by changes in Shh-mediated dorsal-ventral patterning (Figure 4A-J). Expression of ShhN, ShhN-E90A, and ShhN-H183A causes extensive dorsal expansion of the Nkx2.2 and Mnr2 domains (Figure 4A-F), as well as repression of Pax7 (Figure 4G-J). These results support our finding that binding to the canonical (co)-receptors is not a necessary component for activation of the Hh response *in vivo*.

In order to assess more biologically relevant forms of Shh, we electroporated *Shh*, *ShhE90A,* or *ShhH183A* together with *GFP* in developing chick neural tubes. Expression of *Shh* or *ShhE90A* caused an expansion of Nkx2.2 and Mnr2 domains, as well as a repression of Pax7 (Figure 5A, B, E, F, I, J), indicating that these forms of Shh are active. However, electroporation of *ShhH183A* does not result in extensive activation of the pathway (Figure 5C, G, K). It is unclear why ShhH183A is able to activate the pathway *in vitro* but not *in vivo*. One possibility is that the inability of ShhH183A to efficiently undergo autoproteolysis may prevent pathway activation *in vivo*. To test this hypothesis, we assessed ShhC199A, a form of Shh that is unable to undergo autoproteolytic cleavage (Figure 2B) and is unable to mediate signaling *in trans* (Roelink et al., 1995). Electroporation of *ShhC199A* causes an expansion of ventral markers as well as a repression of Pax7 (Figure 5D, H, L). This unanticipated result rejects the hypothesis that the inability of ShhH183A to undergo autoproteolysis is the reason why it is inactive *in vivo*, and this issue remains unresolved. However, the ability of ShhN-E90A, ShhN-183A, and ShhE90A to induce the Hh response in the developing neural tube provides *in vivo* support of our finding that Smo can be activated by ShhN without the need to bind to its canonical (co-)receptors.

We stained electroporated neural tubes with the anti-Shh monoclonal antibody 5E1 (Ericson et al., 1996). 5E1 staining pattern on the (left) side of neural tubes overexpressing *ShhN* or *Shh* coincide with *GFP* expressing cells (Figure 3K and 4M). The 5E1 staining of neural tubes expressing ShhN-E90A and in particular ShhE90A is more profuse than neural tubes expressing ShhN or Shh (Figure 4L and 5N). There are two plausible explanations for this observation. 1) The inability of Shh to bind to the co-receptors could greater access to the 5E1 epitope, or 2) inactivation of the putative cannibalistic protease activity of Shh (Rebollido-Rios et al., 2014) might result in higher steady state levels of ShhE90A. The 5E1 staining pattern on neural tubes expressing ShhN-H183A, ShhH183A and Shh-C199A reveals only endogenous Shh expression in the floor plate (Figure 4M, 5O, and 5P). The discrepancy between the effects on patterning and the absence of 5E1 staining of these mutants is possibly caused by poor recognition of the uncleaved ligand, in combination with the disruption of the epitope in the H183Shh mutant. Importantly, the lack of ectopic 5E1 staining in embryos expressing ShhN-H183A and ShhC199A that show ectopic activation of the Hh response,

demonstrates that the effect on neural tube patterning is mediated by these Shh mutants as such, and not due to secondary induction of endogenous Shh expression.

The cell-autonomous activity of ShhN is unaffected by alternate C-terminal extensions, but is impeded by the cholesterol modification

The observation that the expression of ShhN, which lacks the C-terminal cholesterol modification, is a much more potent activator of the Hh response than Shh led us to assess the extent to which forms of Shh with varying lipophilic and C-terminal modifications can signal cell-autonomously and *in trans*. We evaluated fully modified Shh, as well as forms of Shh lacking either the cholesterol moiety (ShhN), the palmitoyl moiety (ShhC25S), or both (ShhN-C25S) (Bumcrot et al., 1995b; Gao et al., 2011; Pepinsky et al., 1998; Porter et al., 1996) (Figure 5A).

The ability of Shh to signal to *Ptch1*$^{LacZ/LacZ}$;*Ptch2*$^{-/-}$ reporter cells *in trans* (Figure 5A, top diagram) was unaffected by the absence or presence of its lipophilic modifications, with the exception of ShhN-C25S (Figure 5B). The absence of palmitoylation on ShhN results in an inability to signal *in trans*, as observed before (Chen et al., 2004). ShhN with distinct C-terminal extensions have been shown to be active in embryos before: ShhN::CD4 induces digit duplications when expressed in limb buds (Yang et al., 1997), and ShhN::GFP can partially rescue the genetic loss of *Shh* (Chamberlain et al., 2008). Both ShhN::CD4 and ShhN::GFP are membrane bound; ShhN::CD4 by its transmembrane domain in CD4, and ShhN::GFP due a cholesterol moiety at the carboxyterminal end of GFP. Both ShhN::CD4 and ShhN::GFP retain the ability to activate the Hh response *in trans* (Figure 5B). Consistent with previous observations (Roelink et al., 1995), we find that ShhC199A, which is unable to undergo autoproteolytic cleavage, is unable to significantly induce Hh response *in trans*.

The finding that cells expressing wild type *Shh* are poorly responsive to their own signal has been reported before (García-Zaragoza et al., 2012), and consistent with the finding that Shh primarily signals *in trans* (Bailey et al., 2009; Tian et al., 2009). This is in stark contrast to the observation that ShhN is a potent cell-autonomous activator. To evaluate the extent to which the lipophilic modifications of Shh affect its ability to activate the Hh response cell-autonomously, we transfected *Ptch1*$^{LacZ/LacZ}$;*Ptch2*$^{-/-}$ reporter cells with constructs coding for various forms of lipid-modified Shh (Figure 5A, bottom diagram). We find that the palmitoylation of Shh has little effect on its poor ability to induce a cell-autonomous response, unlike its activity *in trans* (Figure 5C). Similarly, preventing palmitoylation of ShhN (ShhN-C25S) does not affect its ability to induce the Hh response cell-autonomously. Interaction between the palmitate of Shh and Ptch1 has shown to be critical for repressing Ptch1-mediated inhibition (Tukachinsky et al., 2016), and thus the ability of ShhN-C25S

to activate the pathway supports the idea that cell-autonomous pathway activation occurs independently of Ptch1/2-mediated inhibition of Smo. This result is further reinforced by the observation that expression of ShhN-C25S causes an upregulation of the Hh response in the developing neural tube (Figure 6, Figure Supplement 1).

The presence of cholesterol on Shh significantly decreases its ability to induce the Hh response cell-autonomously (Figure 6C, 3F, 3I). This decrease in activity is not due to its membrane association, as Shh::CD4 and Shh::GFP are potent cell-autonomous activators of the Hh pathway (Figure 6C). Consistent with the observation that forms of Shh with extraneous C termini are able to induce the Hh response cell-autonomously, we found that the uncleaved ShhC199A mutant also retains the ability to cell-autonomously activate the pathway in *Ptch1*$^{LacZ/LacZ}$;*Ptch2*$^{-/-}$ cells (Figure 6C). These results concur with our observation that ShhC199A can induce the Hh response *in vivo* (Figure 5D, H, L). It appears that an important function of the cholesterol moiety on Shh is to prevent Shh-expressing cells from strongly upregulating the Hh response cell-autonomously. To test whether the cholesterol modification on Shh alters its cellular distribution, we used the 5E1 antibody to stain transfected *Ptch1*$^{LacZ/LacZ}$;*Ptch2*$^{-/-}$ cells for either wildtype Shh or ShhN. We find that Shh is stereotypically localized to the cell membrane, including filopodial extensions (Figure 6D). ShhN is consistently absent from the cell membrane and filopodial structures, and instead occupies a perinuclear location (Figure 6E). This suggests that the processing and subsequent cholesterol modification of Shh regulates its localization within expressing cells, possibly preventing co-localization with Smo or interaction with other proteins. The cholesterol modification biases against the activation of the Hh response in cells that produce Shh, thereby restricting its effects to non-cell autonomous activation of the Hh pathway. Together these results support our observation that many forms of Shh can activate Smo via a mechanism that does not involve any of the known co-receptors.

Discussion

The canonical model of Smo activation mediated by the Shh-induced release of Ptch1 inhibition is challenged by our observations. Despite the ample evidence that Ptch1 is an efficient inhibitor of Smo (Goodrich et al., 1997), we find that the loss of *Ptch1/2* does not inevitably result in maximal Smo activation, and that a variety of Shh mutants can activate the migrational and transcriptional Hh responses in the absence of Ptch1/2 function.

Whether cells lacking Ptch1 or Ptch2 retain sensitivity to Shh *in vivo* is unclear, however some provocative evidence indicates that they might. The spectrum of tumors observed in *Ptch1* null and

in *Ptch1/2* heterozygous mice (Lee et al., 2006), from basal cell carcinomas to medulloblastomas (Goodrich et al., 1997; Lee et al., 2006; Mao et al., 2006), are commonly found at sites where Shh is expressed; and Shh-induced tumors often arise at the same locations (Beachy et al., 2004). According to the canonical model, the loss of Ptch1/2 function should result in the cell-autonomous activation of the Hh response. The positional overlap between tumors induced by the loss of Ptch function and Shh-induced tumors is compatible with our model that cells lacking Ptch1/2 function nevertheless retain some ability to respond to Shh. Our model is further supported by the observation that Smo is required for the establishment of left/right symmetry in mouse embryos, whereas *Ptch1* is not (Zhang et al., 2001b). *Pitx2* expression can be induced by Shh (Ryan et al., 1998), and requires *Smo* as well as *Shh* and *Ihh* (Zhang et al., 2001b). Interestingly, *Ptch1*$^{-/-}$ mutant embryos normally establish asymmetric expression of *Pitx2*, demonstrating that this Hh/Smo-mediated symmetry-breaking event can occur independently of Ptch1. Analysis of *Ptch1*$^{-/-}$;*Ptch2*$^{-/-}$;*Shh*$^{-/-}$;*Ihh*$^{-/-}$ compound null embryos would help to resolve the issue as to what extent the loss of Ptch1/2 activity is epistatic to the loss of Shh and Ihh.

In *Drosophila* embryos, the genetic loss of *Ptch* is epistatic to the loss of *Hh* (Bejsovec and Wieschaus, 1993), suggesting that Ptch-independent regulation of Smo does not play a major role during *Drosophila* development. The incongruity between our data and *Drosophila* genetics may be explained by auxiliary molecules involved in *Drosophila* Smo activation that are present in cells lacking Ptch, creating the impression that loss of Ptch-mediated inhibition unequivocally results in Smo activation. However, our model is consistent with the finding that cells in the posterior compartment of the wing imaginal disc retain responsiveness to the Hh ligand independent of Ptch function (Ramirez-Weber et al., 2000), highlighting a mechanism of Smo activation in *Drosophila* akin to the one we observe in *Ptch1*$^{LacZ/LacZ}$;*Ptch2*$^{-/-}$ cells. It is not terribly surprising that Smo, expressed from a single gene in most vertebrates and invertebrates, would have a complex mechanism of regulation and activation, given that it is responsible for relaying most known Hh responses in the organism.

Our results demonstrate that a wide variety of Shh mutants, many previously characterized as “dead” signals, retain their ability to activate Smo in cell lines lacking the canonical receptors as well as in wildtype cells within developing embryos. Of all the forms of Shh tested, wildtype Shh is unique in that it is unable to induce the cell-autonomous Hh response, while it can still efficiently signal non-cell autonomously. In stark contrast, ShhC199A, which remains unprocessed as a full length precursor, cannot signal to neighboring cells, but is an efficient inducer of the Hh response cell-autonomously. These results indicate that an important function of the unusual processing and modification of Shh is to prevent activation of the Hh response in cells that express the ligand, thus

reinforcing strict non-cell autonomous signaling. The ability of ShhC199A to induce the Hh response autonomously came as a surprise, and this switch between cell-autonomous to non-cell autonomous activity upon cleavage has implications for the understanding of diseases associated with mutations in *Shh*.

Several *Shh* mutations that cause Holoprosencephaly result in forms of Shh that fail to autoproteolytically cleave, which strongly correlates with their inability to induce the Hh response *in trans* (Singh et al., 2009; Traiffort et al., 2004). Moreover, many of the otherwise uncharacterized *SHH* mutants found in patients with Holoprosencephaly are located in the C-terminal domain, and thus possibly affect autoproteolytic cleavage (Roessler et al., 2009). We found that ShhC199A is perfectly capable of inducing the Hh response when expressed in the developing neural tube. It appears that many mutations in the C-terminal domain of SHH could give rise to forms that gain the ability to induce the Hh response cell-autonomously. Heterozygous mutations in the C-terminal domain of *SHH* can cause holoprosencephaly (Hehr et al., 2010); however, mice heterozygous for a null *Shh* allele are normal. Two identified *Shh* mutations that cause Holoprosencephaly change the Cysteine residue at position 198 that is required for Shh processing (homologous to the C199 residue in mice), thus resulting in an obligatory full-length form of Shh (Roessler et al., 2009). Thus, either unprocessed Shh functions as a dominant negative form of Shh, or cell-autonomous activation of the Hh response in cells heterozygous for this mutation contributes to holoprosencephaly. Given our observation that ShhC199A is a potent inducer of the Hh response *in vivo*, we favor the latter explanation.

The data we present here, along with recently published results from our lab (Roberts et al., 2016) and data from the literature, supports a model in which Ptch1/2 mediates the allosteric inhibition of Smo by means of its antiporter function in the absence of the Shh ligand. Upon the availability of Shh in the extracellular space, Shh can bind to a receptor complex via the ligand-binding domain (L2) of Ptch1/2. We hypothesize that this event represses the allosteric inhibition mediated by Ptch1/2 (Figure 7). The Shh ligand is internalized by the receptor complex, resulting in its co-localization with Smo in an endocytic compartment where it mediates an orthosteric activation of (disinhibited) Smo. It is important to stress that Shh-mediated activation may not occur through direct binding to Smo. Although Smo was initially considered to be the putative receptor for Hh when it was identified in *Drosophila*, there has been no evidence to support direct binding between Shh and Smo. Many questions about cell-autonomous Hh activation by Shh are left to be explored, however a central question remains: What is the basis of the interaction between Shh and Smo? A multidisciplinary approach of biochemistry, genetics, and bioinformatics may be required to solve this enduring puzzle.

Materials and Methods

Materials: Vismodegib was a gift from Dr. Fred de Sauvage (Genentech). SAG was from EMD Biochemicals. Recombinant ShhN protein was from R&D Systems. Cell Tracker Green CMFDA was from Invitrogen.

Electroporations: Hamburger-Hamilton (HH) stage 10 Gallus gallus embryos were electroporated caudally in the developing neural tube using standard procedures (Meyer and Roelink, 2003). Embryos were incubated for another 48 h following electroporation, dissected, fixed in 4% PFA, mounted in Tissue-Tek OCT Compound (Sakura) and sectioned.

Embryoid Body differentiation: mESCs were neuralized and differentiated into embryoid bodies (NEBs) using established procedures (Wichterle et al., 2002). NEBs were harvested after 5 days in culture, fixed, and stained for Nkx2.2 and Olig2 (Kawakami et al., 1997). NEBs were mounted in Fluoromount-G (Southern Biotech) and imaged.

Immunofluorescence: Antibodies for mouse Pax7 (1:10), Mnr2 (1:100), Nkx2.2 (1:10), Shh (5E1, 1:20) were from the Developmental Studies Hybridoma Bank. The Rabbit α-GFP (1:1000) antibody was from Invitrogen, and the Goat α-hOlig2 (1:100) antibody was from R&D Systems. The mouse α-acetylated tubulin (1:200) was from Sigma Aldrich. Alexa488 and Alexa568 secondary antibodies (1:1000) were from Invitrogen. Nuclei were stained with DAPI (Invitrogen).

DNA Constructs: The *Gli-Luciferase* reporter and the Renilla control were gifts from Dr. H. Sasaki (Sasaki et al., 1997). *Ptch1* was a gift from Dr. Scott (Stanford University, CA, USA). *Ptch1-Δloop2* was a gift from Dr. Thomas Jessell (Columbia University, NY, USA). *Ptch1* channel mutants were previously described (Alfaro et al., 2014). SmoΔCRD was a gift from J. Reiter (Aanstad et. al., 2009). SmoM2 was from Genentech (F. de Sauvage). The following mutations were created using Quikchange mutagenesis (Stratagene): *Shh-E90A*, *Shh-H183A*, *ShhN-E90A*, *ShhN-H183A*, *SmoΔCRD-CLD*, *SmoL112DW113Y. Shh::GFP* and *Shh::CD4* were gifts from Dr. Andrew McMahon (University of Southern California, CA, USA). Dhh and Ihh were gifts from Charles Emerson Jr. (University of Massachusetts Medical School, MA, USA). *DhhN* and *IhhN* were made by site directed mutagenesis of C199 (Dhh) and C203 (Ihh) to a stop codon. ShhC199A was previously described (Roelink et al., 1995). $Gli3^{PHS}$ was previously described (Meyer et. al., 2003).

Genome Editing: TALEN constructs targeting the first exon of mouse Cdo and Gas1 were designed and cloned into the pCTIG expression vectors containing IRES puromycin and IRES hygromycin selectable markers (Cermak et al., 2011). The following repeat variable domain sequences were

generated: Cdo, 5' TALEN: NN HD NI NG HD HD NI NN NI HD HD NG HD NN NN ; 3' TALEN: HD NI HD NI NI NN NI NI HD NI NG NI HD NI NN; Gas1, 5' TALEN: NN NI NN NN NI HD NN HD HD HD NI NG NN HD HD; 3' TALEN: NN NN NI NI NI NI NN NG NG NG NN NG HD HD NN NI. Two CRISPR constructs targeting a double strand break flanking the first exon of mouse Boc were cloned into pSpCas9 vector with an IRES puromycin selectable marker (Ran et al., 2013). The Boc CRISPRs targeted the following forward genomic sequences (PAM sequences underlined): Upstream of first exon 5' CCTGTCCTCGCTGTTGGTCCCTA 3'; Downstream of first exon 5' CCCACAGACTCGCTGAAGAGCTC 3'. *Ptch1*$^{LacZ/LacZ}$*;Ptch2*$^{-/-}$*;Shh*$^{-/-}$ mouse embryonic stem cells (Roberts et al., 2016) were plated at a density of 1.0x106 on 6-well plates and transfected with 6 genome editing plasmids the following day. One day after transfection, selective ES medium (100 µg/mL hygromycin and 0.5 µg/mL puromycin) was added for 4 days. Selective medium was removed and surviving mESC colonies were isolated, expanded and genotyped by sequence PCR products spanning TALEN and CRISPR-binding sites.

Genotyping: PCR screening was performed on cell lysates using primers flanking the TALEN or CRISPR binding sites for the *Boc*, *Cdo*, and *Gas1* loci. *Boc*, (5') CATCTAACAGCGTTGTCCAACAATG and (3') CAAGGTGGTATTGTCCGGATC; *Cdo*, (5') CACTTCAGTGTGATCTCCAG and (3') CCTTGAACTCACAGAGATTCG; Gas1, (5') ATGCCAGAGCTGCGAAGTGCTA and (3') AGCGCCTGCCAGCAGATGAG. PCR products were sequenced. Samples with signals indicative of INDEL mutations were cloned into the pCR-BluntII vector using the Zero Blunt TOPO PCR cloning kit (Invitrogen) and sequenced to confirm allele sequences. A *Ptch1*$^{LacZ/LacZ}$;*Ptch2*$^{-/-}$;*Boc*$^{-/-}$;*Cdo*$^{-/-}$;*Gas1*$^{-/-}$*;Shh*$^{-/-}$ mESC clone was identified harboring a 50 bp deletion in Cdo exon 1, a heteroallelic 480 bp insertion and a 200 bp deletion in Gas1 exon1 resulting in a premature stop codon in the reading frame, and a 450 bp deletion of Boc exon 1.

Cell Culture: *Ptch1*$^{LacZ/LacZ}$*;Ptch2*$^{-/-}$, *Ptch1*$^{LacZ/LacZ}$*;Ptch2*$^{-/-}$;*Smo*$^{-/-}$, *Ptch1*$^{-/-}$*;Disp1*$^{-/-}$*;Shh*$^{-/-}$, and *Ptch1*$^{LacZ/LacZ}$;*Ptch2*$^{-/-}$;*Boc*$^{-/-}$;*Cdo*$^{-/-}$;*Gas1*$^{-/-}$*;Shh*$^{-/-}$ fibroblasts were obtained by plating mESCs at a density of 8.0x10^5 cells in 6-well plates and transfected with the *large T antigen* from the SV40 virus (Gökhan et al., 1998) in ES medium. Cells were then switched to DMEM (Invitrogen) supplemented with 10% fetal bovine serum (FBS) without LIF. *Ptch1*$^{+/LacZ}$ and *Ptch1*$^{LacZ/LacZ}$ fibroblasts (gifts from Dr. Scott) were cultured in DMEM supplemented with 10% FBS (Invitrogen) and maintained under standard conditions. Identity of these lines was confirmed by the presence of the LacZ recombination in the Ptch1 locus, the presence of 40 chromosomes per cell, and mouse-specific DNA sequences of the edited genes. mESC lines were maintained using standard conditions in dishes coated with gelatin, without feeder cells. Cells were routinely tested for Mycoplasm by Hoechst stain, and grown in the presence of tetracycline and gentamycin at regular intervals. Cultures with visible Mycoplasma

infection were discarded. None of the cell lines used in this study is listed in the Database of Cross-Contaminated or Misidentified Cell Lines. Fibroblast-like lines derived from the mESCs were re-sequenced at the edited loci to confirm their identity.

Transfection: Cells were transiently transfected for 24h at 80-90% confluency using Lipofectamine 2000 reagent (Invitrogen) according to the manufacturer's protocol.

Modified Boyden Chamber Migration Assay: Cell migration assays were performed as previously described (Bijlsma et. al. 2007). Cells were labeled with 10 μM CellTracker Green (Invitrogen) in DMEM for one hour. The well compartments were set up with the specified chemoattractant (ShhN .75 μg/ML (resuspended in 0.1%BSA in PBS), 10% FCS, or no attractant (plus 0.1%BSA in PBS) and pre-warmed at 37˚C. Cells were then detached with 5mM EDTA and resuspended in DMEM without phenol red and supplemented with 50mM HEPES. Cells were transferred into FluoroBlok Transwell inserts (BD Falcon) at $5.0x10^4$ cells per insert. GFP-spectrum fluorescence in the bottom compartment was measured every 2 min for 99 cycles (approximately 3 hours), after which background fluorescence (medium without cells) and a no-attractant control was subtracted from each time point. Starting points of migration were set to 0.

Gli-Luciferase Assay: Fibroblasts were plated at a density of $3x10^4$ in 24 well plates and transfected with *Gli-Luciferase*, *CMV-Renilla* (control plasmid), and specified plasmids 24 hours after plating. Cells were grown to confluency and then switched to low serum medium (0.5% FBS) alone or with specified concentrations of Vismodegib or SAG. After 24 hours, cells were lysed and the luciferase activity in lysates was measured using the Dual Luciferase Reporter Assay System (Promega). Raw Luciferase values were normalized against Renilla values for each biological replicate to control against variation in transfection efficiency. Individual luciferase/renilla values were then normalized against the mock control average for each experiment.

LacZ Assay: Fibroblasts were plated at a density of $3x10^4$ in 24 well plates and transfected with plasmids 24 hours after plating (or remained untransfected for SAG experiments). Fibroblasts were grown to confluency and then switched to a low serum medium (0.5% FBS) alone or with specified concentrations of Vismodegib or SAG. After 24 hours, cells were lysed and lysates were analyzed using the Galacto-Light™ chemiluminescence kit (Applied Biosciences) for level of LacZ expression. Raw chemiluminescence values were normalized against total protein for each biological replicate. Protein concentration was determined with a Bradford assay using the Bio-Rad Protein Assay Dye Reagent.

Co-Culture Assay: *Ptch1*$^{LacZ/LacZ}$;*Ptch2*$^{-/-}$ reporter cells were plated at a density of $1.4X10^5$ in 6-well plates and transfected with *Gli-Luciferase*, *CMV-Renilla*, and with or without a variant of *Ptch1* 24

hours after plating. *Ptch1*$^{LacZ/LacZ}$;*Ptch2*$^{-/-}$ signaling cells were plated similarly and transfected with a variant of Shh 24 hours after plating. Cells were then trypsinized and plated in 24-well plates in specified combinations ($1.5x10^4$ of each type) 24 hours after transfections. Cells were grown to confluency and switched to low serum medium (0.5% FBS) for 16 hours before assaying for luciferase activity.

Western Blots: *Ptch1*$^{LacZ/LacZ}$;*Ptch2*$^{-/-}$ cells were transfected with Shh mutants as indicated. 48 hours after transfection, *Ptch1*$^{LacZ/LacZ}$;*Ptch2*$^{-/-}$ cells were rinsed with PBS and lysed with RIPA buffer (150 mM NaCl, 50 mM Tris-Hcl, 1% Igepal, 0.5% Sodium Deoxycholate, and protease inhibitors) for 30 min on ice. Protein lysate was cleared by centrifugation at 13,000g for 30 min at 4 °C. 20 µg of each sample was run on a 15% SDS-PAGE gel and transferred to a 0.45 micron nitrocellulose membrane. Membranes were blocked with 5% milk in Tris-buffered saline with 0.1% Tween-20 (TBS-T) and incubated with a rabbit polyclonal anti-Shh antibody (H160; Santa Cruz Biotechnology) at 1:250. A goat anti-rabbit HRP-conjugated secondary antibody (Biorad) was used at 1:10000.

Acknowledgements: This work was supported by NIH grants R01GM097035 and 1R01GM117090 to HR. Vismodegib was a gift from Dr. de Sauvage (Genentech), *Dhh* and *Ihh* were a gift from Dr. Charles P. Emerson III (U. Mass. Med. School). Dr. A. Alfaro cloned the Shh binding mutants (E90A, H183A) and made the initial observation that they activate the Hh pathway *in vivo*. We thank Dr. M. Barro for her help with Western blotting, Dr. M. F. Bijlsma (AMC Amsterdam) for his help with the migration assays, and Dr. B. Roberts (Allen Institute for Cell Science) for his comments and advice. We also thank Fatma Ozguc for help with genome editing of the *Ptch1*$^{LacZ/LacZ}$;*Ptch2*$^{-/-}$;*Boc*$^{-/-}$;*Cdo*$^{-/-}$;*Gas1*$^{-/-}$;*Shh*$^{-/-}$ mESC line.

Author contributions: CC performed all experiments. HR and CC designed the experiments and wrote the manuscript.

References

Aanstad, P., Santos, N., Corbit, K.C., Scherz, P.J., Trinh le, A., Salvenmoser, W., Huisken, J., Reiter, J.F., and Stainier, D.Y. (2009). The extracellular domain of Smoothened regulates ciliary localization and is required for high-level Hh signaling. Curr. Biol. *19*, 1034–1039.

Alfaro, A.C., Roberts, B., Kwong, L., Bijlsma, M.F., and roelink, H. (2014). Ptch2 mediates the Shh response in Ptch1-/- cells. Development (Cambridge, England).

Allen, B.L., Song, J.Y., Izzi, L., Althaus, I.W., Kang, J.S., Charron, F., Krauss, R.S., and McMahon, A.P. (2011). Overlapping roles and collective requirement for the coreceptors GAS1, CDO, and BOC in SHH pathway function. Developmental Cell *20*, 775–787.

Bailey, J.M., Mohr, A.M., and Hollingsworth, M.A. (2009). Sonic hedgehog paracrine signaling regulates metastasis and lymphangiogenesis in pancreatic cancer. Oncogene *28*, 3513–3525.

Bale, A.E. (2002). Hedgehog signaling and human disease. Annu Rev Genomics Hum Genet *3*, 47–65.

Beachy, P.A., Karhadkar, S.S., and Berman, D.M. (2004). Tissue repair and stem cell renewal in carcinogenesis. Nature *432*, 324–331.

Bejsovec, A., and Wieschaus, E. (1993). Segment polarity gene interactions modulate epidermal patterning in Drosophila embryos. Development (Cambridge, England) *119*, 501–517.

Bhanot, P., Brink, M., Samos, C.H., Hsieh, J.C., Wang, Y., Macke, J.P., Andrew, D., Nathans, J., and Nusse, R. (1996). A new member of the frizzled family from Drosophila functions as a Wingless receptor. Nature *382*, 225–230.

Bijlsma, M.F., Damhofer, H., and roelink, H. (2012). Hedgehog-stimulated chemotaxis is mediated by smoothened located outside the primary cilium. Sci Signal *5*, ra60.

593 Briscoe, J., Chen, Y., Jessell, T.M., and Struhl, G. (2001). A hedgehog-insensitive form of patched
594 provides evidence for direct long-range morphogen activity of sonic hedgehog in the neural tube.
595 Molecular Cell *7*, 1279–1291.

596 Bumcrot, D.A., Takada, R., and McMahon, A.P. (1995a). Proteolytic processing yields two secreted
597 forms of sonic hedgehog. Mol. Cell. Biol. *15*, 2294–2303.

598 Bumcrot, D.A., Takada, R., and McMahon, A.P. (1995b). Proteolytic processing yields two secreted
599 forms of sonic hedgehog. Mol. Cell. Biol. *15*, 2294–2303.

600 Byrne, E.F.X., Sircar, R., Miller, P.S., Hedger, G., Luchetti, G., Nachtergaele, S., Tully, M.D.,
601 Mydock-McGrane, L., Covey, D.F., Rambo, R.P., et al. (2016). Structural basis of Smoothened
602 regulation by its extracellular domains. Nature *535*, 517–522.

603 Cermak, T., Doyle, E.L., Christian, M., Wang, L., Zhang, Y., Schmidt, C., Baller, J.A., Somia, N.V.,
604 Bogdanove, A.J., and Voytas, D.F. (2011). Efficient design and assembly of custom TALEN and
605 other TAL effector-based constructs for DNA targeting. Nucleic Acids Res. *39*, e82.

606 Chamberlain, C.E., Jeong, J., Guo, C., Allen, B.L., and McMahon, A.P. (2008). Notochord-derived
607 Shh concentrates in close association with the apically positioned basal body in neural target cells
608 and forms a dynamic gradient during neural patterning. Development (Cambridge, England) *135*,
609 1097–1106.

610 Chen, H.C. (2005). Boyden chamber assay. Methods in Molecular Biology (Clifton, N.J *294*, 15–22.

611 Chen, J.K., Taipale, J., Cooper, M.K., and Beachy, P.A. (2002a). Inhibition of Hedgehog signaling
612 by direct binding of cyclopamine to Smoothened. Genes & Development *16*, 2743–2748.

613 Chen, J.K., Taipale, J., Young, K.E., Maiti, T., and Beachy, P.A. (2002b). Small molecule
614 modulation of Smoothened activity. Proceedings of the National Academy of Sciences of the
615 United States of America *99*, 14071–14076.

616 Chen, M.H., Li, Y.J., Kawakami, T., Xu, S.M., and Chuang, P.T. (2004). Palmitoylation is required
617 for the production of a soluble multimeric Hedgehog protein complex and long-range signaling in
618 vertebrates. Genes Dev. *18*, 641–659.

619 Corbit, K.C., Aanstad, P., Singla, V., Norman, A.R., Stainier, D.Y., and Reiter, J.F. (2005).
620 Vertebrate Smoothened functions at the primary cilium. Nature *437*, 1018–1021.

621 Ericson, J., Morton, S., Kawakami, A., Roelink, H., and Jessell, T.M. (1996). Two critical periods of
622 Sonic Hedgehog signaling required for the specification of motor neuron identity. Cell *87*, 661–673.

623 Fuse, N., Maiti, T., Wang, B., Porter, J.A., Hall, T.M., Leahy, D.J., and Beachy, P.A. (1999). Sonic
624 hedgehog protein signals not as a hydrolytic enzyme but as an apparent ligand for patched.
625 Proceedings of the National Academy of Sciences of the United States of America *96*, 10992–
626 10999.

627 Gao, X., Arenas-Ramirez, N., Scales, S.J., and Hannoush, R.N. (2011). Membrane targeting of
628 palmitoylated Wnt and Hedgehog revealed by chemical probes. FEBS Letters *585*, 2501–2506.

629 García-Zaragoza, E., Pérez-Tavarez, R., Ballester, A., Lafarga, V., Jiménez-Reinoso, A., Ramírez,
630 A., Murillas, R., and Gallego, M.I. (2012). Intraepithelial paracrine Hedgehog signaling induces the
631 expansion of ciliated cells that express diverse progenitor cell markers in the basal epithelium of

the mouse mammary gland. Developmental Biology *372*, 28–44.

Goetz, J.A., Singh, S., Suber, L.M., Kull, F.J., and Robbins, D.J. (2006). A highly conserved amino-terminal region of sonic hedgehog is required for the formation of its freely diffusible multimeric form. J. Biol. Chem. *281*, 4087–4093.

Goodrich, L.V., Milenkovic, L., Higgins, K.M., and Scott, M.P. (1997). Altered neural cell fates and medulloblastoma in mouse patched mutants. Science (New York, N.Y *277*, 1109–1113.

Gökhan, S., Song, Q., and Mehler, M.F. (1998). Generation and regulation of developing immortalized neural cell lines. Methods *16*, 345–358.

Hamburger, V., and Hamilton, H.L. (1951). A series of normal stages in the development of the chick embryo. J. Morphol. *88*, 49–90.

Hehr, U., Pineda-Alvarez, D.E., Uyanik, G., Hu, P., Zhou, N., Hehr, A., Schell-Apacik, C., Altus, C., Daumer-Haas, C., Meiner, A., et al. (2010). Heterozygous mutations in SIX3 and SHH are associated with schizencephaly and further expand the clinical spectrum of holoprosencephaly. Hum. Genet. *127*, 555–561.

Huang, P., Nedelcu, D., Watanabe, M., Jao, C., Kim, Y., Liu, J., and Salic, A. (2016). Cellular Cholesterol Directly Activates Smoothened in Hedgehog Signaling. Cell *166*, 1176–1187.e14.

Incardona, J.P., Gruenberg, J., and Roelink, H. (2002). Sonic hedgehog induces the segregation of patched and smoothened in endosomes. Curr. Biol. *12*, 983–995.

Incardona, J.P., Lee, J.H., Robertson, C.P., Enga, K., Kapur, R.P., and Roelink, H. (2000). Receptor-mediated endocytosis of soluble and membrane-tethered Sonic hedgehog by Patched-1. Proc. Natl. Acad. Sci. U.S.a. *97*, 12044–12049.

Ingham, P.W., and McMahon, A.P. (2001). Hedgehog signaling in animal development: paradigms and principles. Genes & Development *15*, 3059–3087.

Itasaki, N., Bel-Vialar, S., and Krumlauf, R. (1999). “Shocking” developments in chick embryology: electroporation and in ovo gene expression. Nature Cell Biology *1*, E203–E207.

Izzi, L., Levesque, M., Morin, S., Laniel, D., Wilkes, B.C., Mille, F., Krauss, R.S., McMahon, A.P., Allen, B.L., and Charron, F. (2011). Boc and Gas1 each form distinct Shh receptor complexes with Ptch1 and are required for Shh-mediated cell proliferation. Developmental Cell *20*, 788–801.

Janda, C.Y., Waghray, D., Levin, A.M., Thomas, C., and Garcia, K.C. (2012). Structural basis of Wnt recognition by Frizzled. Science (New York, N.Y *337*, 59–64.

Kawakami, A., Kimura Kawakami, M., Nomura, T., and Fujisawa, H. (1997). Distributions of PAX6 and PAX7 proteins suggest their involvement in both early and late phases of chick brain development. Mechanisms of Development *66*, 119–130.

Kristiansen, K. (2004). Molecular mechanisms of ligand binding, signaling, and regulation within the superfamily of G-protein-coupled receptors: molecular modeling and mutagenesis approaches to receptor structure and function. Pharmacol Ther *103*, 21–80.

Lee, Y., Miller, H.L., Russell, H.R., Boyd, K., Curran, T., and McKinnon, P.J. (2006). Patched2 modulates tumorigenesis in patched1 heterozygous mice. Cancer Research *66*, 6964–6971.

Mao, J., Ligon, K.L., Rakhlin, E.Y., Thayer, S.P., Bronson, R.T., Rowitch, D., and McMahon, A.P. (2006). A novel somatic mouse model to survey tumorigenic potential applied to the Hedgehog pathway. Cancer Research *66*, 10171–10178.

Marigo, V., Davey, R.A., Zuo, Y., Cunningham, J.M., and Tabin, C.J. (1996). Biochemical evidence that patched is the Hedgehog receptor. Nature *384*, 176–179.

Meyer, N.P., and Roelink, H. (2003). The amino-terminal region of Gli3 antagonizes the Shh response and acts in dorsoventral fate specification in the developing spinal cord. Developmental Biology *257*, 343–355.

Milenkovic, L., Scott, M.P., and Rohatgi, R. (2009). Lateral transport of Smoothened from the plasma membrane to the membrane of the cilium. The Journal of Cell Biology *187*, 365–374.

Myers, B.R., Sever, N., Chong, Y.C., Kim, J., Belani, J.D., Rychnovsky, S., Bazan, J.F., and Beachy, P.A. (2013). Hedgehog pathway modulation by multiple lipid binding sites on the smoothened effector of signal response. Developmental Cell *26*, 346–357.

Nachtergaele, S., Whalen, D.M., Mydock, L.K., Zhao, Z., Malinauskas, T., Krishnan, K., Ingham, P.W., Covey, D.F., Siebold, C., and Rohatgi, R. (2013). Structure and function of the Smoothened extracellular domain in vertebrate Hedgehog signaling. Elife *2*, e01340.

Nedelcu, D., Liu, J., Xu, Y., Jao, C., and Salic, A. (2013). Oxysterol binding to the extracellular domain of Smoothened in Hedgehog signaling. Nature Chemical Biology.

Nikaido, H., and Zgurskaya, H.I. (2001). AcrAB and related multidrug efflux pumps of Escherichia coli. Journal of Molecular Microbiology and Biotechnology *3*, 215–218.

Nikaido, H., and Takatsuka, Y. (2009). Mechanisms of RND multidrug efflux pumps. Biochimica Et Biophysica Acta *1794*, 769–781.

Okada, A., Charron, F., Morin, S., Shin, D.S., Wong, K., Fabre, P.J., Tessier-Lavigne, M., and McConnell, S.K. (2006). Boc is a receptor for sonic hedgehog in the guidance of commissural axons. Nature *444*, 369–373.

Pepinsky, R.B., Zeng, C., Wen, D., Rayhorn, P., Baker, D.P., Williams, K.P., Bixler, S.A., Ambrose, C.M., Garber, E.A., Miatkowski, K., et al. (1998). Identification of a palmitic acid-modified form of human Sonic hedgehog. The Journal of Biological Chemistry *273*, 14037–14045.

Porter, J.A., Young, K.E., and Beachy, P.A. (1996). Cholesterol modification of hedgehog signaling proteins in animal development. Science (New York, N.Y *274*, 255–259.

Ramirez-Weber, F.A., Casso, D.J., Aza-Blanc, P., Tabata, T., and Kornberg, T.B. (2000). Hedgehog signal transduction in the posterior compartment of the Drosophila wing imaginal disc. Molecular Cell *6*, 479–485.

Ran, F.A., Hsu, P.D., Wright, J., Agarwala, V., Scott, D.A., and Zhang, F. (2013). Genome engineering using the CRISPR-Cas9 system. Nat Protoc *8*, 2281–2308.

Rebollido-Rios, R., Bandari, S., Wilms, C., Jakuschev, S., Vortkamp, A., Grobe, K., and Hoffmann, D. (2014). Signaling domain of Sonic Hedgehog as cannibalistic calcium-regulated zinc-peptidase. PLoS Comput. Biol. *10*, e1003707.

Roberts, B., Casillas, C., Alfaro, A.C., Jägers, C., and roelink, H. (2016). Patched1 and Patched2 inhibit Smoothened non-cell autonomously. Elife *5*, e17634.

Roelink, H., Porter, J.A., Chiang, C., Tanabe, Y., Chang, D.T., Beachy, P.A., and Jessell, T.M. (1995). Floor plate and motor neuron induction by different concentrations of the amino-terminal cleavage product of sonic hedgehog autoproteolysis. Cell *81*, 445–455.

Roessler, E., El-Jaick, K.B., Dubourg, C., Vélez, J.I., Solomon, B.D., Pineda-Alvarez, D.E., Lacbawan, F., Zhou, N., Ouspenskaia, M., Paulussen, A., et al. (2009). The mutational spectrum of holoprosencephaly-associated changes within the SHH gene in humans predicts loss-of-function through either key structural alterations of the ligand or its altered synthesis. Hum. Mutat. *30*, E921–E935.

Rohatgi, R., Milenkovic, L., and Scott, M.P. (2007). Patched1 regulates hedgehog signaling at the primary cilium. Science (New York, N.Y *317*, 372–376.

Rudin, C.M. (2012). Vismodegib. Clin. Cancer Res. *18*, 3218–3222.

Ryan, A.K., Blumberg, B., Rodriguez-Esteban, C., Yonei-Tamura, S., Tamura, K., Tsukui, T., la Peña, de, J., Sabbagh, W., Greenwald, J., Choe, S., et al. (1998). Pitx2 determines left-right asymmetry of internal organs in vertebrates. Nature *394*, 545–551.

Sasaki, H., Hui, C., Nakafuku, M., and Kondoh, H. (1997). A binding site for Gli proteins is essential for HNF-3beta floor plate enhancer activity in transgenics and can respond to Shh in vitro. Development (Cambridge, England) *124*, 1313–1322.

Singh, S., Tokhunts, R., Baubet, V., Goetz, J.A., Huang, Z.J., Schilling, N.S., Black, K.E., MacKenzie, T.A., Dahmane, N., and Robbins, D.J. (2009). Sonic hedgehog mutations identified in holoprosencephaly patients can act in a dominant negative manner. Hum. Genet. *125*, 95–103.

Taipale, J., Cooper, M.K., Maiti, T., and Beachy, P.A. (2002). Patched acts catalytically to suppress the activity of Smoothened. Nature *418*, 892–897.

Tenzen, T., Allen, B.L., Cole, F., Kang, J.S., Krauss, R.S., and McMahon, A.P. (2006). The cell surface membrane proteins Cdo and Boc are components and targets of the Hedgehog signaling pathway and feedback network in mice. Developmental Cell *10*, 647–656.

Tian, H., Callahan, C.A., DuPree, K.J., Darbonne, W.C., Ahn, C.P., Scales, S.J., and de Sauvage, F.J. (2009). Hedgehog signaling is restricted to the stromal compartment during pancreatic carcinogenesis. Proceedings of the National Academy of Sciences of the United States of America *106*, 4254–4259.

Traiffort, E., Dubourg, C., Faure, H., Rognan, D., Odent, S., Durou, M.-R., David, V., and Ruat, M. (2004). Functional characterization of sonic hedgehog mutations associated with holoprosencephaly. J. Biol. Chem. *279*, 42889–42897.

Tukachinsky, H., Petrov, K., Watanabe, M., and Salic, A. (2016). Mechanism of inhibition of the tumor suppressor Patched by Sonic Hedgehog. Proceedings of the National Academy of Sciences of the United States of America *113*, E5866–E5875.

Wang, Y., and McMahon, A.P. (2013). A novel site comes into sight. Elife *2*, e01680.

Wichterle, H., Lieberam, I., Porter, J.A., and Jessell, T.M. (2002). Directed differentiation of

747 embryonic stem cells into motor neurons. Cell *110*, 385–397.

748 Xie, J., Murone, M., Luoh, S.M., Ryan, A., Gu, Q., Zhang, C., Bonifas, J.M., Lam, C.W., Hynes, M.,
749 Goddard, A., et al. (1998). Activating Smoothened mutations in sporadic basal-cell carcinoma.
750 Nature *391*, 90–92.

751 Yang, Y., Drossopoulou, G., Chuang, P.T., Duprez, D., Marti, E., Bumcrot, D., Vargesson, N.,
752 Clarke, J., Niswander, L., McMahon, A., et al. (1997). Relationship between dose, distance and
753 time in Sonic Hedgehog-mediated regulation of anteroposterior polarity in the chick limb.
754 Development (Cambridge, England) *124*, 4393–4404.

755 Zhang, J., Rosenthal, A., de Sauvage, F.J., and Shivdasani, R.A. (2001a). Downregulation of
756 Hedgehog signaling is required for organogenesis of the small intestine in Xenopus.
757 Developmental Biology *229*, 188–202.

758 Zhang, X.M., Ramalho-Santos, M., and McMahon, A.P. (2001b). Smoothened mutants reveal
759 redundant roles for Shh and Ihh signaling including regulation of L/R asymmetry by the mouse
760 node. Cell *105*, 781–792.

761

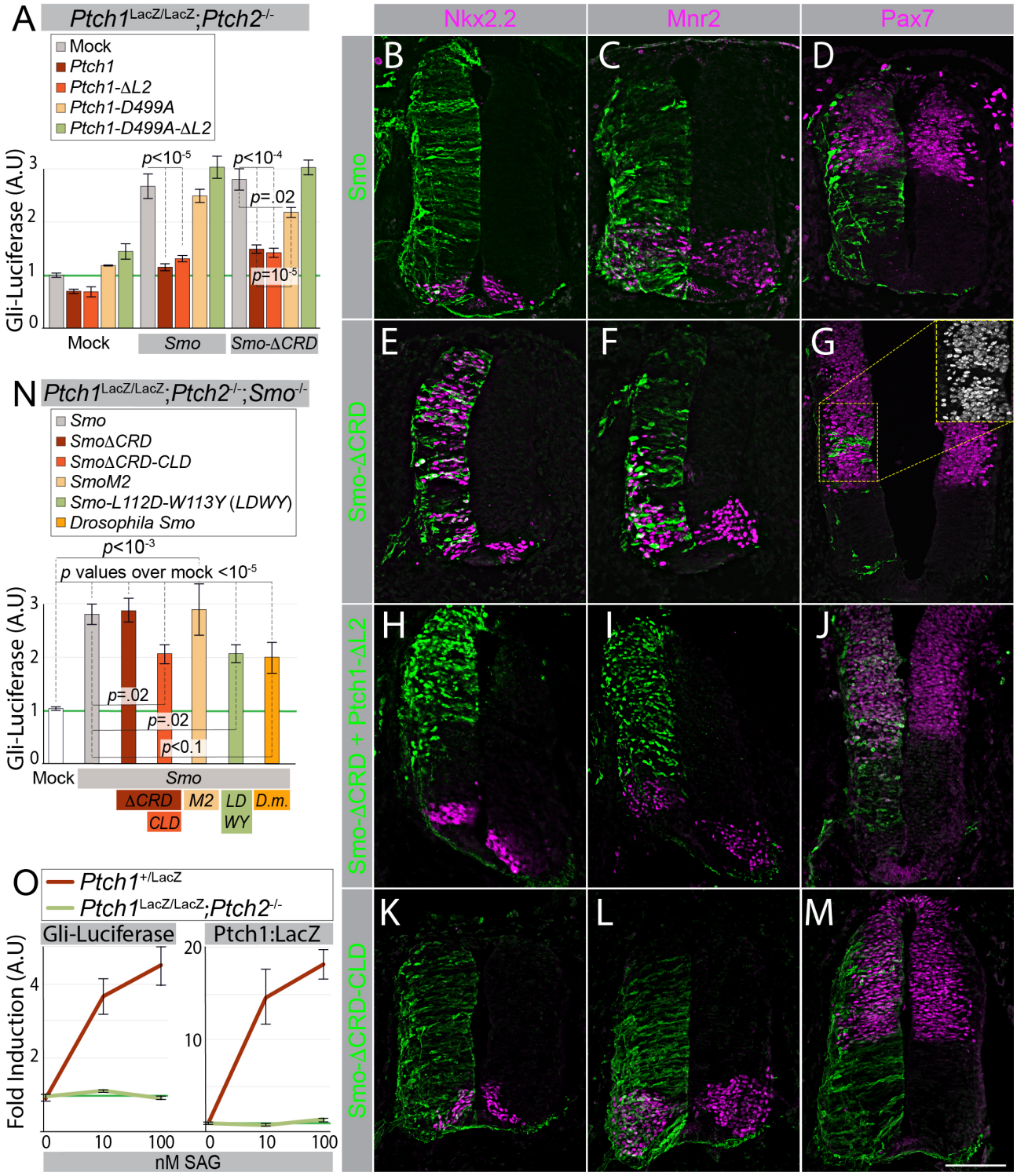

762

763 **Figure 1. SmoΔCRD retains sensitivity to Ptch1-mediated inhibition in vitro and in vivo**

764 (A) *Ptch1*$^{LacZ/LacZ}$;*Ptch2*$^{-/-}$ cells were co-transfected with *Gli-luc* and *GFP* (Mock), *Ptch1*, *Ptch1-ΔL2*,

765 *Ptch1-D499A*, or *Ptch1ΔL2-D499A*; or *Gli-luc*, *Smo*, and *GFP*, *Ptch1*, *Ptch1-ΔL2*, *Ptch1D499A*, or

766 *Ptch1-ΔL2-D499A*; or *Gli-luc*, *Smo-ΔCRD* and *GFP*, *Ptch1*, *Ptch1-ΔL2*, *Ptch1-D499A*, or *Ptch1-ΔL2-*
767 *D499A*. Luciferase levels in *Gli-luc* Mock transfected *Ptch1*$^{LacZ/LacZ}$;*Ptch2*$^{-/-}$ cells were arbitrarily set at
768 "1". (B-M) Cross-sections of stage 20 HH chicken neural tubes electroporated with *Smo* (B-D), *Smo-*
769 *ΔCRD* (E-G), *Smo-ΔCRD* + *Ptch1-ΔL2* (1:1) (H-J), or *Smo-ΔCRD-CLD* (K-M) labeled in green.
770 Sections are stained with antibodies to Nkx2.2 (B, E, H, K), Mnr2 (C, F, I, L), and Pax7 (D, G, J, M)
771 labeled in magenta. Insert in G shows Pax7 staining. Scale bar is 100μm. (N) *Ptch1*$^{LacZ/LacZ}$;*Ptch2*$^{-/-}$
772 ;*Smo*$^{-/-}$ fibroblasts were co-transfected with *Gli-luc* and the indicated Smo variant. Luciferase levels
773 in *Gli-luc* Mock transfected *Ptch1*$^{LacZ/LacZ}$;*Ptch2*$^{-/-}$;*Smo*$^{-/-}$ cells were arbitrarily set at "1". (O) SAG dose-
774 response in *Ptch1*$^{+/LacZ}$ and *Ptch1*$^{LacZ/LacZ}$;*Ptch2*$^{-/-}$. The Hh response was measured by transfected
775 *Gli-luc*, or by measuring LacZ levels from the *Ptch1:LacZ* allele. Pathway activation in the absence
776 of SAG was set at "1". All error bars are s.e.m., *p* values (Student T-test, 2 tailed) are indicated were
777 relevant, (A) n≥4, (N) n≥4, (O) n≥4, all independent biological replicates.

778

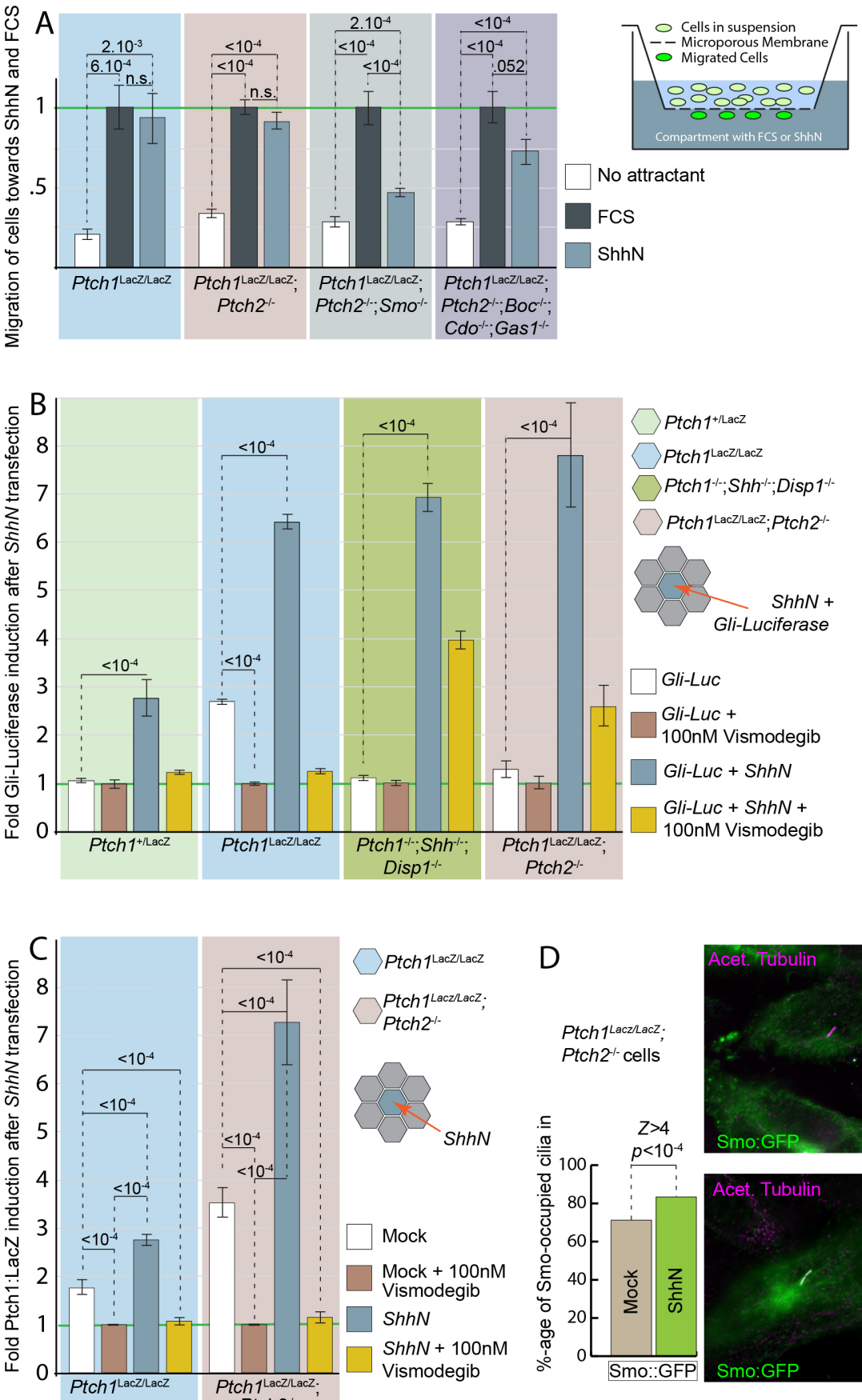

Figure 2. Activation of the Hh response by ShhN does not require Ptch1/2 activity

(A) Cells with the indicated genotypes were assayed in a modified Boyden chamber (diagram) for their ability to migrate towards FCS or ShhN. Migration was normalized to FCS for each condition. (B) *Ptch1*$^{+/LacZ}$ cells, *Ptch1*$^{LacZ/LacZ}$ cells, *Ptch1*$^{-/-}$;*Shh*$^{-/-}$;*Disp1*$^{-/-}$, and *Ptch1*$^{LacZ/LacZ}$;*Ptch2*$^{-/-}$ cells (indicated) were co-transfected with *Gli-Luc* and *GFP* (Mock; white/brown bars) or co-transfected with *Gli-Luc* and *ShhN* (blue/yellow bars). Each condition was treated with either a Smo inhibitor, 100 nM Vismodegib (brown/yellow bars), or a DMSO vehicle control (white/blue bars). Luciferase levels in mock transfected cells treated with 100 nM Vismodegib for each cell line were set at "1". (C) *Ptch1*$^{LacZ/LacZ}$ cells and *Ptch1*$^{LacZ/LacZ}$;*Ptch2*$^{-/-}$ (indicated) were assessed for Ptch1:LacZ expression after mock transfection (white/brown bars) or *ShhN* transfection (blue/yellow bars). Each condition was treated with either a Smo inhibitor, 100 nM Vismodegib (brown/yellow bars), or a DMSO vehicle control (white/blue bars). Luciferase levels in mock transfected cells treated with 100 nM Vismodegib for each cell line were set at "1". (D) Cilial localization of Smo::GFP was quantified in Mock and *ShhN* transfected *Ptch1*$^{LacZ/LacZ}$;*Ptch2*$^{-/-}$ cells. Over 300 Smo::GFP co-expressing cells were assessed for each condition. Z (standard) score>4, *p*-value is $<10^{-4}$. All error bars are s.e.m., *p* values (Student T-test, 1 tailed) are indicated were relevant, (A) n≥4, (B) n≥9, (C) n≥13, all independent biological replicates.

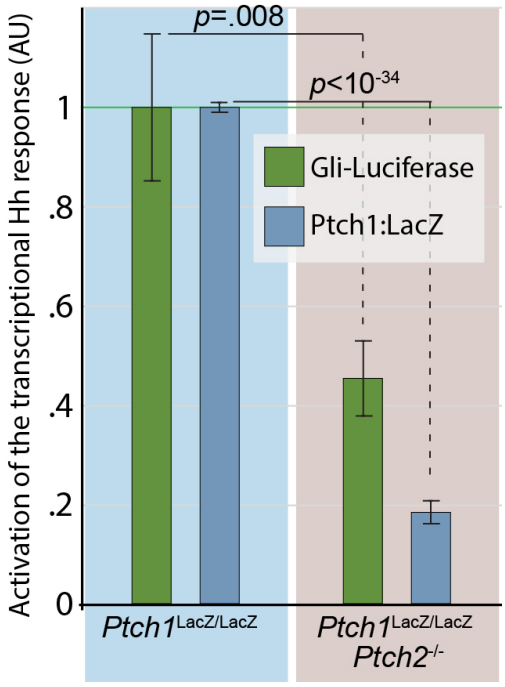

798

799 **Figure 2, Figure Supplement 1. Intrinsic levels of Hh pathway activation in *Ptch1*$^{LacZ/LacZ}$ and**
800 ***Ptch1*$^{LacZ/LacZ}$;*Ptch2*$^{-/-}$ cells.** Hh pathway activation in *Ptch1*$^{LacZ/LacZ}$ and *Ptch1*$^{LacZ/LacZ}$;*Ptch2*$^{-/-}$ was
801 measured in parallel using *Gli-luc* and *Ptch1:LacZ.* Using both methods we find higher Hh pathway
802 activation in the *Ptch1*$^{LacZ/LacZ}$ cells than the *Ptch1*$^{LacZ/LacZ}$;*Ptch2*$^{-/-}$ cells. Luciferase and LacZ levels in
803 *Ptch1*$^{LacZ/LacZ}$ cells were set at "1". Error bars are s.e.m., *p*-values (Student t-test, 2 tailed) are
804 indicated were relevant, n=6 for Gli-Luc assay, n≥25 for LacZ assay, all independent biological
805 replicates.

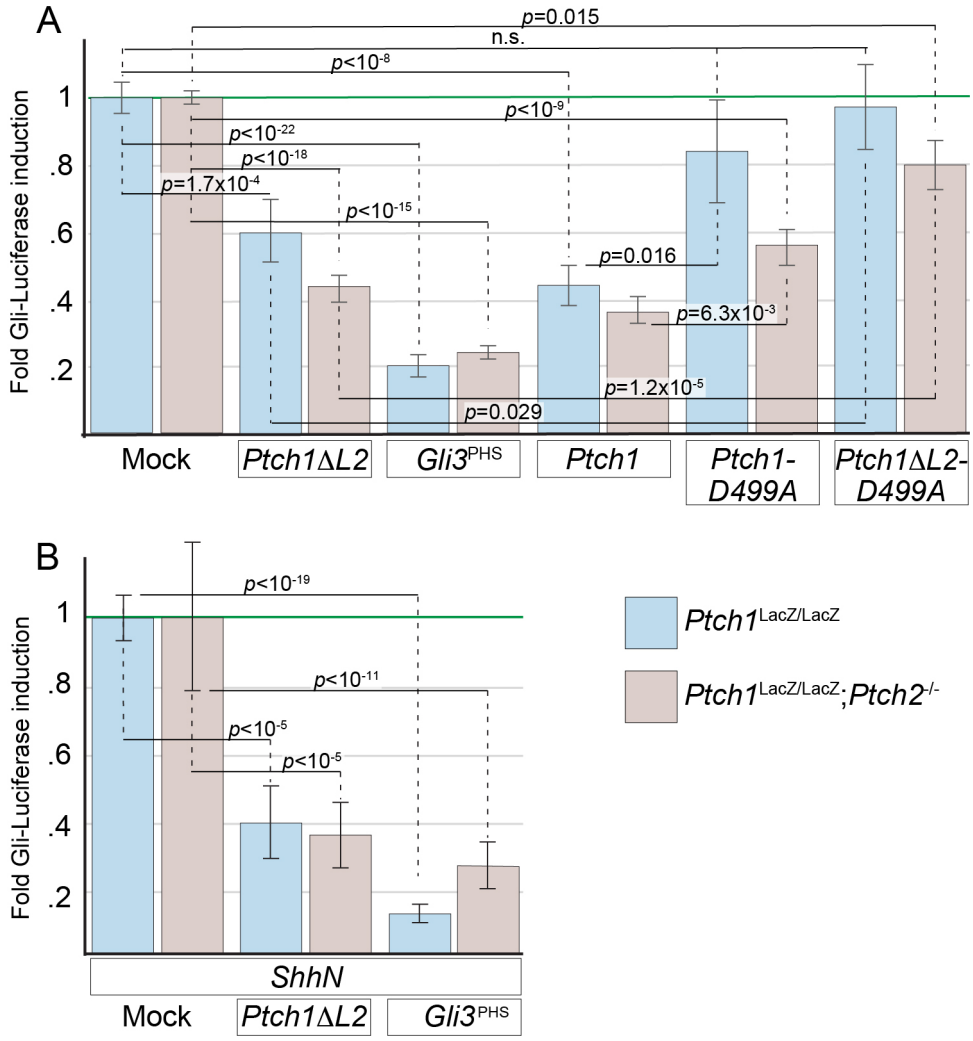

Figure 2, Figure Supplement 2. Ptch1-mediated inhibition of the Hh response is similar in *Ptch1*$^{LacZ/LacZ}$ and *Ptch1*$^{LacZ/LacZ}$;*Ptch2*$^{-/-}$ cells. (A) Gli-luc levels were assayed in *Ptch1*$^{LacZ/LacZ}$ (blue bars) and *Ptch1*$^{LacZ/LacZ}$;*Ptch2*$^{-/-}$ (pink bars) transfected with *Ptch1*, *Ptch1ΔL2*, *Ptch1-D499A*, *Ptch1ΔL2-D499A* (indicated) or a dominant inhibitory form of *Gli3* (*Gli3*^{phs}) together with *Gli-luc*. Luciferase levels in *Gli-Luc* Mock transfected cells were set at "1" for each cell line. (B) Gli-luc levels were assayed in *Ptch1*$^{LacZ/LacZ}$ (blue bars) and *Ptch1*$^{LacZ/LacZ}$;*Ptch2*$^{-/-}$ (pink bars) transfected with *Ptch1ΔL2*,*or Gli3*^{phs} together with *Gli-luc* and *ShhN*. Luciferase levels in *ShhN*, Mock co-transfected cells were set at "1" for each cell line. All error bars are s.e.m., *p*-values (Student t-test, 2 tailed) are indicated were relevant, (A) n≥4, (B) n≥11, all independent biological replicates.

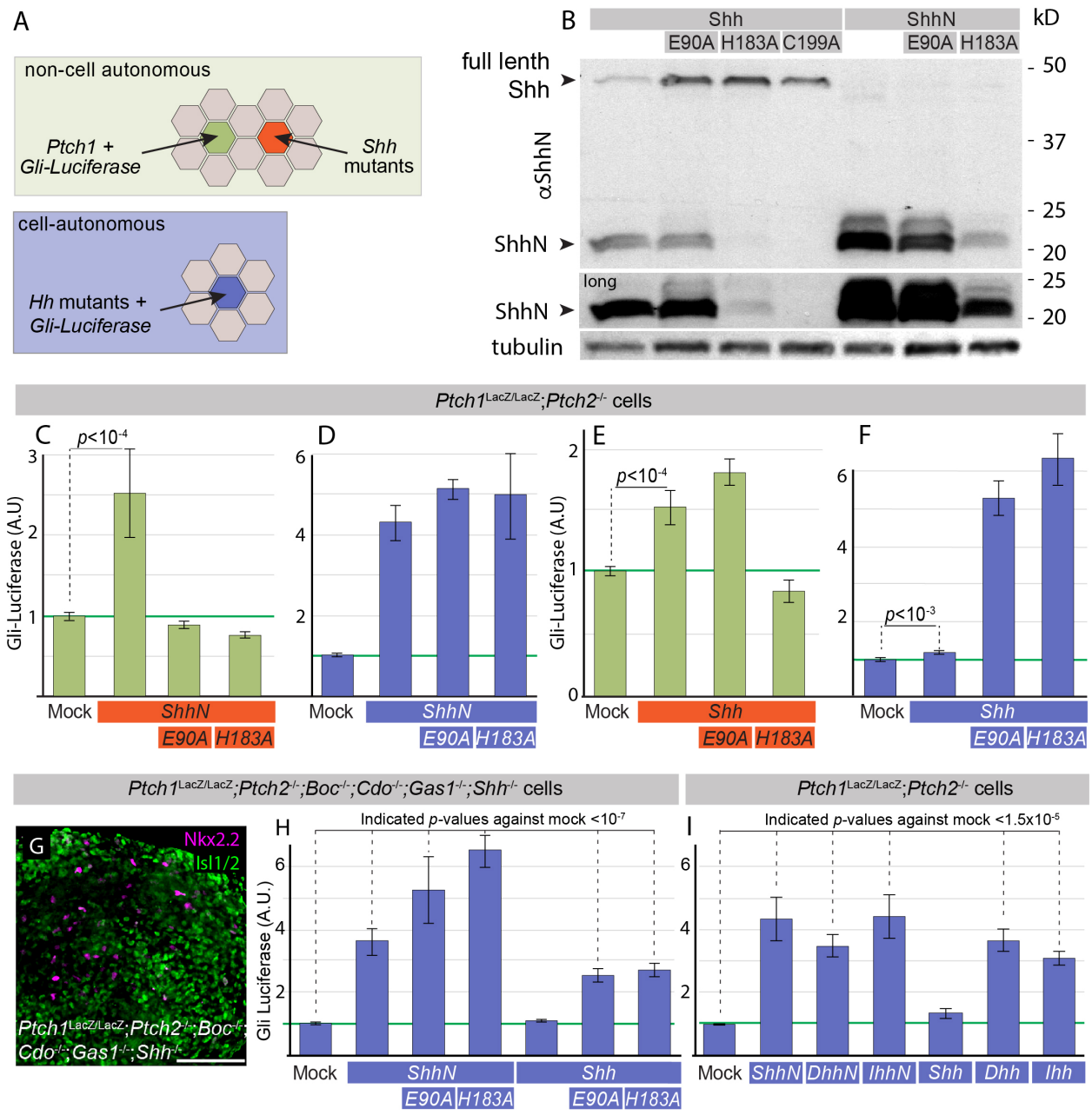

Figure 3. Shh mutants activate the Hh pathway cell-autonomously in cells lacking Hh receptors

(A) Diagram of non-cell autonomous signaling (green background): *Ptch1*$^{LacZ/LacZ}$;*Ptch2*$^{-/-}$ reporter cells transfected with *Gli-Luc* and *Ptch1* (green hexagons) were grown in a 1:1 mixed co-culture of *GFP* (Mock) transfected or *Shh* mutant transfected *Ptch1*$^{LacZ/LacZ}$;*Ptch2*$^{-/-}$ cells (red hexagons). Diagram of cell-autonomous signaling (purple background): *Ptch1*$^{LacZ/LacZ}$;*Ptch2*$^{-/-}$ cells transfected with *Gli-Luc* alone (Mock) or co-transfected with *Shh* mutants. (B) Western blot analysis of Shh, Shh-E90A, Shh-H183A, Shh-C199A, ShhN, ShhN-E90A, and ShhN-H183A protein expression in

827 *Ptch1*$^{LacZ/LacZ}$;*Ptch2*$^{-/-}$ cells, using an antibody directed against the N-terminal domain of Shh. (C)
828 *Ptch1*$^{LacZ/LacZ}$;*Ptch2*$^{-/-}$ reporter cells co-transfected with *Gli-Luc* and *Ptch1* were co-cultured with mock,
829 *ShhN*, *ShhN-E90A*, or *ShhN-H183A* transfected *Ptch1*$^{LacZ/LacZ}$;*Ptch2*$^{-/-}$ cells. Luciferase levels in
830 *Ptch1*$^{LacZ/LacZ}$;*Ptch2*$^{-/-}$ reporter cells co-cultured with mock transfected cells were set at "1". (D)
831 *Ptch1*$^{LacZ/LacZ}$;*Ptch2*$^{-/-}$ cells were transfected with *Gli-Luc* alone (Mock) or co-transfected with *Gli-Luc*
832 and *ShhN*, *ShhN-E90A*, or *ShhN-H183A*. Luciferase levels in mock transfected *Ptch1*$^{LacZ/LacZ}$;*Ptch2*$^{-/-}$
833 cells were set at "1". (E) *Ptch1*$^{LacZ/LacZ}$;*Ptch2*$^{-/-}$ reporter cells co-transfected with *Gli-Luc* and *Ptch1*
834 were co-cultured with mock, *Shh*, *Shh-E90A*, or *Shh-H183A* transfected *Ptch1*$^{LacZ/LacZ}$;*Ptch2*$^{-/-}$ cells.
835 Luciferase levels in *Ptch1*$^{LacZ/LacZ}$;*Ptch2*$^{-/-}$ reporter cells co-cultured with mock transfected cells were
836 set at "1". (F) *Ptch1*$^{LacZ/LacZ}$;*Ptch2*$^{-/-}$ cells were transfected with *Gli-Luc* alone (Mock) or co-transfected
837 with *Gli-Luc* and *Shh*, *Shh-E90A*, or *Shh-H183A*. Luciferase levels in mock transfected
838 *Ptch1*$^{LacZ/LacZ}$;*Ptch2*$^{-/-}$ cells were set at "1". (G) Neuralized Embryoid body derived from
839 *Ptch1*$^{LacZ/LacZ}$;*Ptch2*$^{-/-}$;*Boc*$^{-/-}$;*Cdo*$^{-/-}$;*Gas1*$^{-/-}$;*Shh*$^{-/-}$ mESCs. Expression of Nkx2.2 and Olig2 was
840 assessed by immunofluorescence after 5 days in culture. (H) *Ptch1*$^{LacZ/LacZ}$;*Ptch2*$^{-/-}$;*Boc*$^{-/-}$;*Cdo*$^{-/-}$;*Gas1*$^{-/-}$;*Shh*$^{-/-}$
841 cells were transfected with *Gli-Luc* alone (Mock) or co-transfected with *Gli-Luc* and *Shh*, *Shh-*
842 *E90A*, *Shh-H183A*, *ShhN*, *ShhN-E90A*, or *ShhN-H183A*. Luciferase levels in Mock transfected cells
843 were set at "1". (I) *Ptch1*$^{LacZ/LacZ}$;*Ptch2*$^{-/-}$ cells were transfected with *Gli-Luc* alone (Mock) or co-
844 transfected with *Gli-Luc* and *ShhN*, *DhhN*, *IhhN*, *Shh*, *Dhh*, *or Ihh.* Luciferase levels in Mock
845 transfected cells were set at "1". All error bars are s.e.m., *p* values (Student t-test, 2 tailed) against
846 mock are indicated were relevant, (C) n≥11, (D) n≥25, (E) n≥6, (F) n≥34, (H) n≥4, (I) n≥6, all
847 independent biological replicates.

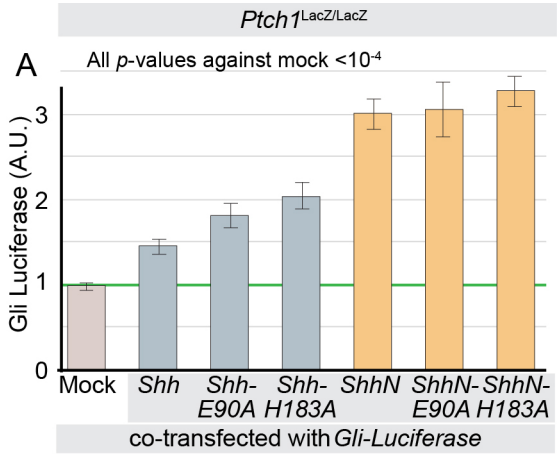

Figure 3, Figure Supplement 1. *Ptch1*$^{LacZ/LacZ}$*;Ptch2*$^{-/-}$ cells activate the Hh response after transfection with Shh mutants (A) *Ptch1*$^{LacZ/LacZ}$ cells were transfected with *Gli-Luc* alone (Mock) or co-transfected with *Gli-Luc* and *Shh*, *Shh-E90A*, *Shh-H183*, *ShhN*, *ShhN-E90A*, or *ShhN-H183A*. Luciferase levels in mock transfected *Ptch1*$^{LacZ/LacZ}$ cells were set at "1". All error bars are s.e.m., *p* values (Student T-test, 2 tailed) are indicated were relevant, n≥5, all independent biological replicates.

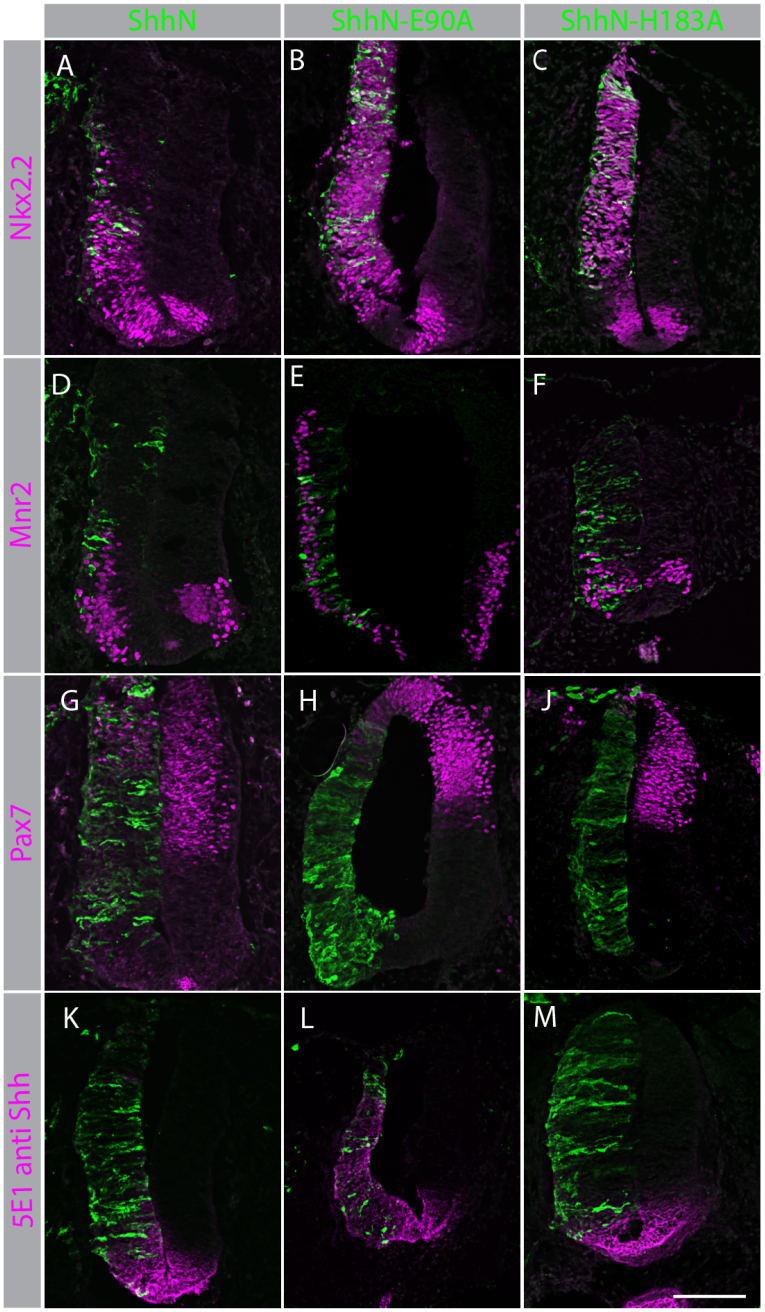

Figure 4. ShhN mutants cell-autonomously activate the Hh pathway *in vivo* independent of extracellular receptor binding

(A-M) Cross-sections of stage 20 HH chicken neural tubes co-electroporated at stage 10 with *GFP* and *ShhN* (A,D,G,K), *ShhN-E90A* (B,E,H,L), or *ShhN-H183A* (C,F,J,M) labeled in green. Sections are stained with antibodies to Nkx2.2 (A-C), Mnr2 (D-F), Pax7 (G-J), and Shh (5E1) (K-M) labeled in magenta. Scale bar is 100μm.

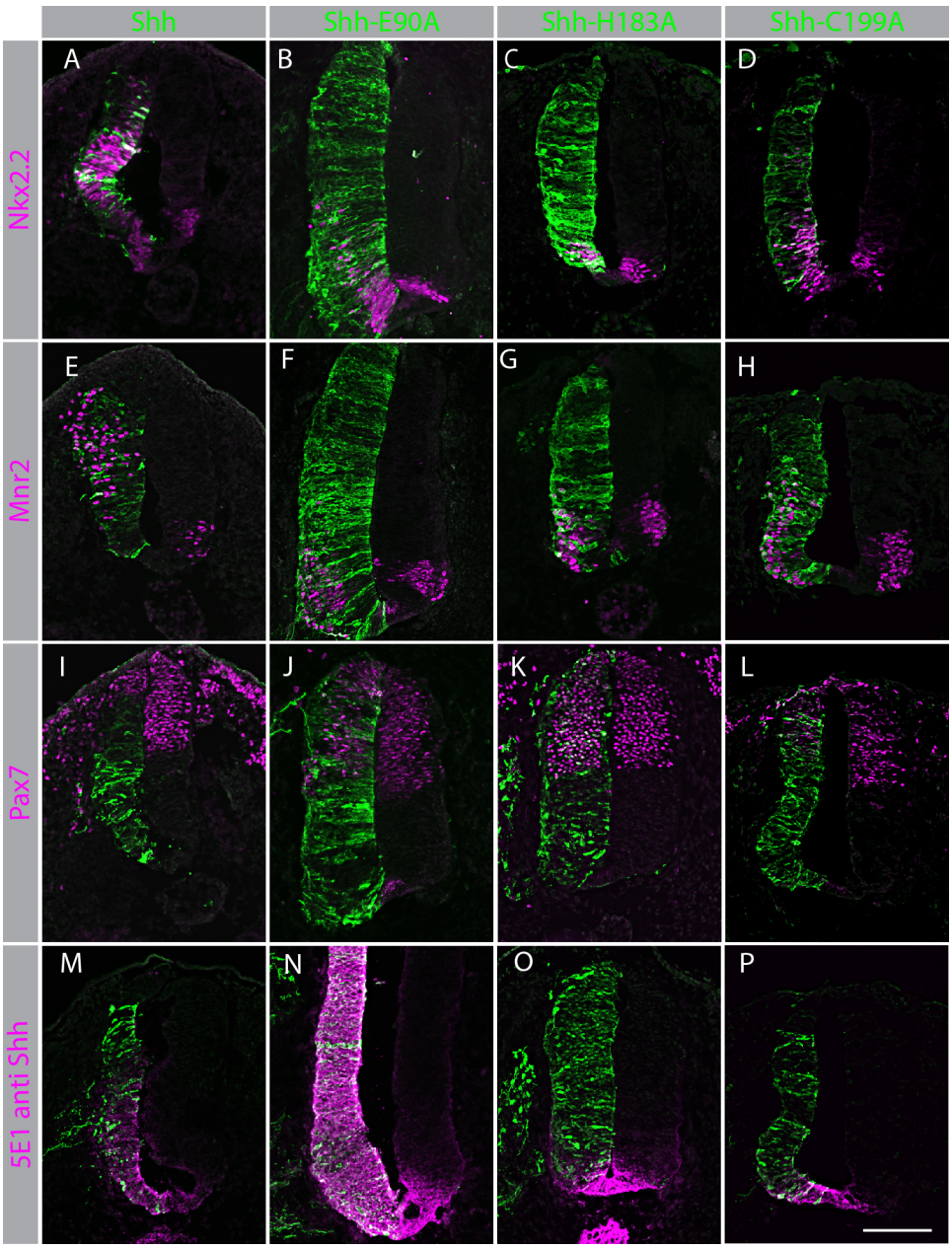

Figure 5. Shh mutants cell-autonomously activate the Hh pathway *in vivo* independent of extracellular receptor binding and despite lack of autoproteolytic processing

(A-P) Cross-sections of stage 20 HH chicken neural tubes co-electroporated with *GFP* and *Shh* (A, E, I, M), *Shh-E90A* (B, F, J, N), *Shh-H183A* (C, G, K, O), or *Shh-C199A* (*C199Ah* (D, H, L, P), labeled in green). Sections are stained with antibodies to Nkx2.2 (A-D), Mnr2 (E-H), Pax7 (I-L), and Shh (5E1) (M-P) labeled in magenta. Scale bar is 100μm.

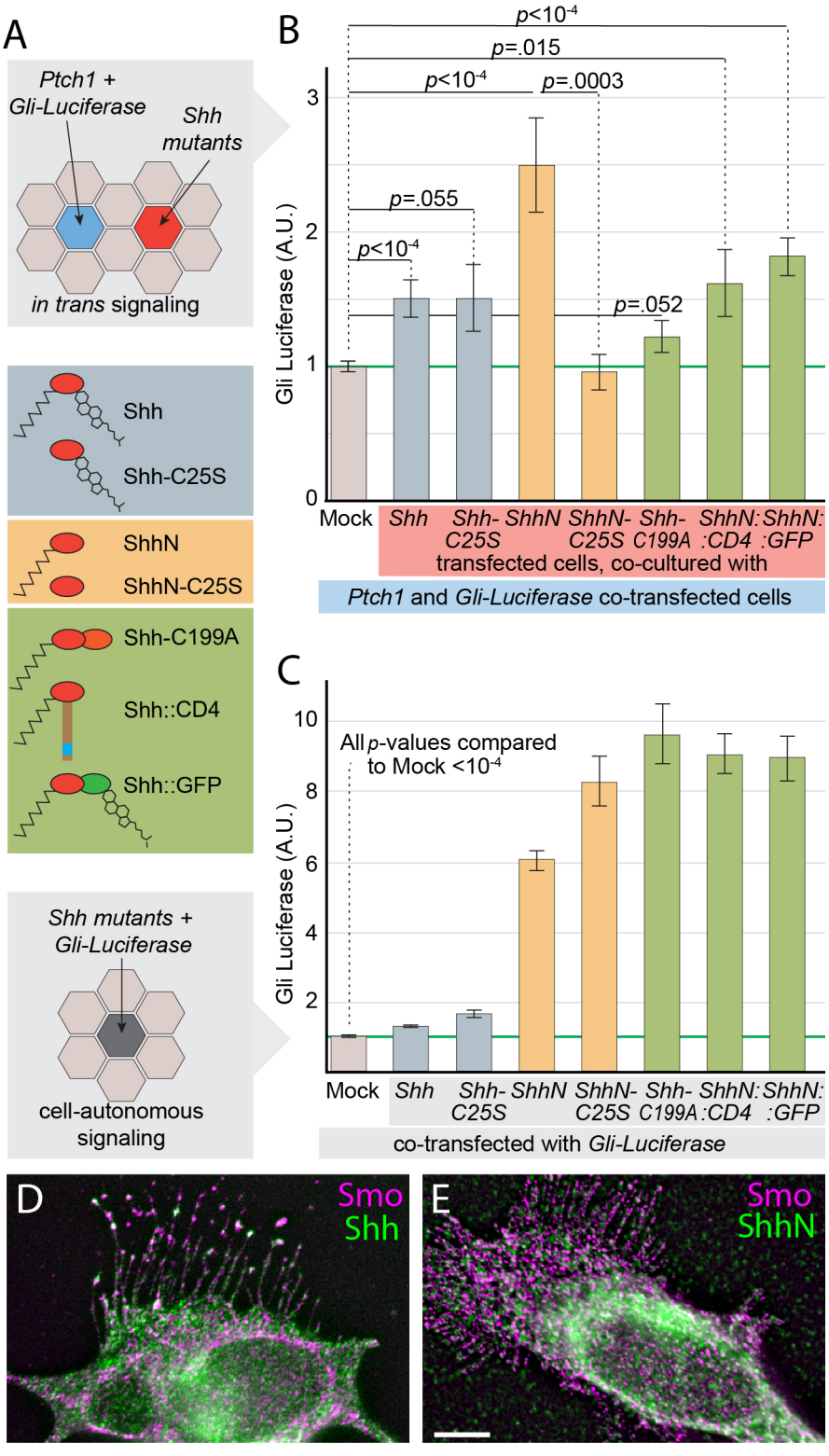

Figure 6. The cholesterol modification of Shh impedes cell-autonomous Hh pathway activation

(A) Diagram of non-cell autonomous signaling (top): *Ptch1*$^{LacZ/LacZ}$;*Ptch2*$^{-/-}$ reporter cells transfected with *Gli-Luc* and *Ptch1* (blue hexagons) were grown in a 1:1 mixed co-culture of *GFP* (Mock) transfected or *Shh* (mutant) transfected *Ptch1*$^{LacZ/LacZ}$;*Ptch2*$^{-/-}$ cells (red hexagons). Cell-autonomous signaling experimental design (bottom): *Ptch1*$^{LacZ/LacZ}$;*Ptch2*$^{-/-}$ cells co-transfected with *Gli-Luc* and *GFP* (Mock) transfected or co-transfected with *Gli-Luc* and *Shh* (mutants). Diagram of Shh (mutants) with varying lipophilic an C-terminal modifications (middle). (B) *Ptch1*$^{LacZ/LacZ}$;*Ptch2*$^{-/-}$ reporter cells transfected with *Gli-Luc* and *Ptch1* were co-cultured with mock, *Shh*, *ShhC25S*, *ShhN*, *ShhN-C25S*, *Shh-C199A*, *Shh:CD4*, or *Shh:GFP* transfected *Ptch1*$^{LacZ/LacZ}$;*Ptch2*$^{-/-}$ cells. Luciferase levels in *Ptch1*$^{LacZ/LacZ}$;*Ptch2*$^{-/-}$ reporter cells co-cultured with Mock transfected cells were set at “1”. (C) *Ptch1*$^{LacZ/LacZ}$;*Ptch2*$^{-/-}$ cells were Mock transfected or transfected with *Shh*, *Shh-C25S*, *ShhN*, *ShhN-C25S*, *Shh-C199A*, *Shh:CD4*, or *Shh:GFP.* Luciferase levels in Mock transfected *Ptch1*$^{LacZ/LacZ}$;*Ptch2*$^{-/-}$ cells were set at “1”. (D) *Ptch1*$^{LacZ/LacZ}$;*Ptch2*$^{-/-}$ cells were transfected with *Shh* and *Smo-myc*. Cells were stained for Shh (5E1) (green) and myc (magenta). (E) *Ptch1*$^{LacZ/LacZ}$;*Ptch2*$^{-/-}$cell transfected with *ShhN* and *Smo-myc*. Cells were stained for ShhN (5E1)(green) and myc (magenta). Scale bar is 20μm. All error bars are s.e.m., *p* values (Student T-test, 2 tailed) are indicated were relevant, (B) n ≥9, (C) n≥8, all independent biological replicates.

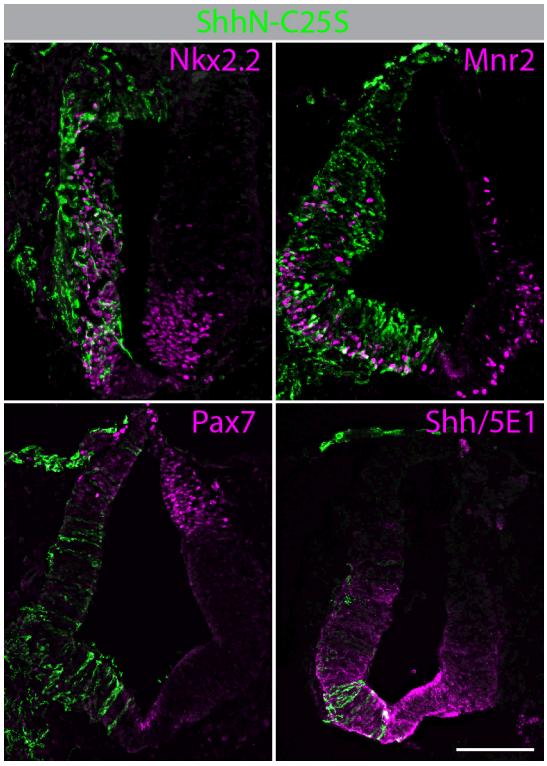

Figure 6, Figure Supplement 1. ShhN-C25S activates the Hh response pathway in vivo

Cross-sections of stage 20 HH chicken neural tubes co-electroporated with *GFP* and *ShhN-C25S* labeled in green. Sections were stained with antibodies to Nkx2.2, Mnr2, Pax7, and Shh (5E1) labeled in magenta. Scale bar is 100μm.

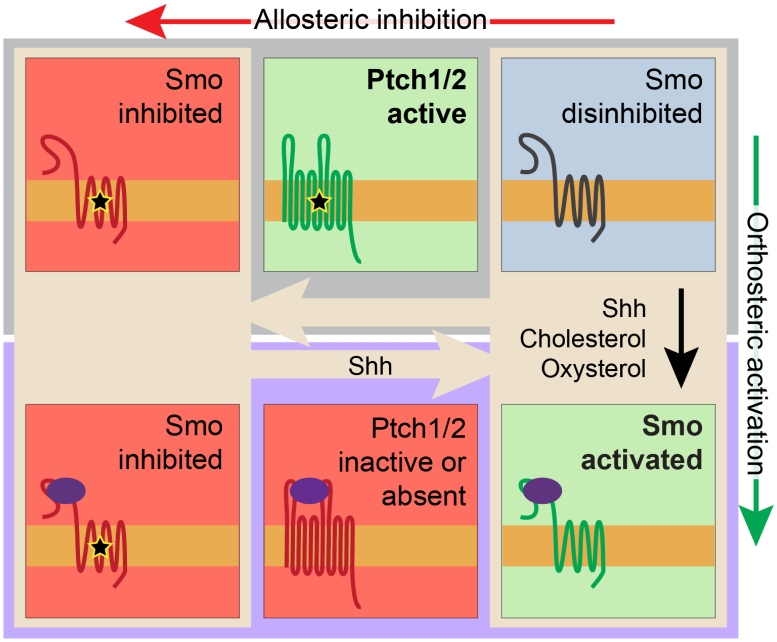

899

900

901 **Figure 7. Model**

902 The absence of Shh ligand from the extracellular environment permits the Ptch1/2-mediated
903 allosteric modulation of Smo activity Ptch1/2 (red arrow) through the transportation of an inhibitor
904 (yellow lined black asterisk) that binds to the heptahelical site on Smo. Shh ligand (purple) in the a
905 Ptch1/2 containing receptor complex on the cell membrane via the Shh binding (L2) domain (blue
906 pictogram), causing the inhibition of Smo to be repressed. This allows the accumulation of
907 disinhibited, inactive Smo (top right). This form of Smo is sensitive to (indirect), orthosteric activation
908 by Shh in a Ptch1/2-independent manner (green arrow).